**Universidade do Minho**
Escola de Medicina

Ana Catarina Barbosa Matos

# Lung fibrosis regulation by c-Met-expressing immune cells

# Regulação da fibrose pulmonar pela expressão de c-Met em células imunes

julho de 2018

Lung fibrosis regulation by c-Met-expressing immune cells
Regulação da fibrose pulmonar pela expressão de c-Met em células imunes
Ana Catarina Barbosa Matos

UMinho | 2018

**Universidade do Minho**
Escola de Medicina

Ana Catarina Barbosa Matos

# Lung fibrosis regulation by c-Met-expressing immune cells

# Regulação da fibrose pulmonar pela expressão de c-Met em células imunes

Dissertação de Mestrado
Mestrado em Ciências da Saúde

Trabalho efetuado sob a orientação da
**Doutora Sandra Maria Araújo da Costa**

julho de 2018

*"Nada na vida deve ser temido,*
*Somente compreendido.*
*Agora é hora de compreender mais para temer menos."*

*Marie Curie*

À minha orientadora e aos indispensáveis na minha vida: pais, avós e namorado,

# Agradecimentos

Estes dois anos revelaram-se uma superação constante, cheia de novos desafios e aprendizagens, possibilitando-me um grande aperfeiçoamento a nível técnico e científico. Esta tese foi possível devido a um grande esforço, dedicação e cooperação, e não seria possível sem todos os que me acompanharam ao longo deste intenso percurso.

Para começar, deixo um enorme agradecimento à Doutora Sandra Costa, por toda a confiança depositada em mim, todo o apoio, todas as oportunidades e sem esquecer todos os sermões construtivos e indispensáveis que me permitiram ultrapassar todas as inseguranças. Senti que valeu a pena ter aceite este desafio e que as expetativas foram superadas, apesar de todas as adversidades.

Antes de mais agradeço às melhores companheiras que levo para a vida, Carol e Sofia, por todas as maratonas de trabalho no laboratório, por todo o apoio, amizade e sobretudo por tornarem os meus dias mais felizes. Sem vocês ao meu lado, com certeza não teria chegado ao fim, obrigada por tudo!

A todos os membros do domínio das ciências cirúrgicas em especial a todos os membros do I1.03 e às meninas que me acompanharam na integração, Filipa Santos e Cristina Freitas.

Aos colegas e amigos que o mestrado me deu, por todos os momentos que partilhamos, pelo companheirismo, pelo apoio e carinho que recebi, um enorme obrigada! Em especial à Diana, à Eduarda, à Sónia, à Nathalia, à Andreia, à Marta e ao Tiago que desde o início me acompanharam e apoiaram, por toda a preocupação e por todo o carinho nos momentos mais difíceis.

Aos velhos colegas e eternos amigos, Patrícia, Tânia, Cláudio, Rita, Ana, Cátia, que sempre me acompanharam neste percurso académico e demonstraram uma constante preocupação e carinho.

À minha família, deixo o agradecimento mais especial por acreditarem nas minhas capacidades e me ajudarem a não baixar os braços, embora sem perceberem a dedicação e entrega que esta tese exigiu. Sem vocês eu não tinha chegado onde cheguei, nem seria a pessoa que sou hoje, muito obrigada do fundo do coração por me darem esta oportunidade e por acreditarem em mim!

E por fim aos amigos de sempre e especialmente ao meu namorado, principalmente por toda a paciência e incentivo, todos os momentos, conversas intermináveis, carinho, dedicação e preocupação que sempre demonstraram e espero um dia poder retribuir porque vocês merecem.

O trabalho apresentado nesta dissertação de tese foi realizado no Instituto de Investigação em Ciências da Vida e Saúde (ICVS), Universidade do Minho.

O financiamento para a realização deste projeto provém dos fundos do Programa Operacional Regional do Norte (NORTE 2020), sobre o Acordo de Parceria PORTUGAL 2020, através do Fundo Europeu de Desenvolvimento Regional (FEDER). O financiamento da FEDER advém também do Programa Operacional Fatores de Competitividade – COMPETE, e dos fundos nacionais através da Fundação para a Ciência e Tecnologia sobre POCI-01-0145-FEDER-007038; e sobre o projeto NORTE-01-0145-FEDER-000013.









# Abstract

Idiopathic pulmonary fibrosis (IPF) is a rapid debilitating lung disease, the most common and lethal form of interstitial lung diseases, which causes remain unknown. Currently, there is no medical therapy capable of reverse the disease progression. This disease comprises a chronic inflammation, where neutrophil-derived proteases have been described as key mediators of tissue damage and consequently decline of lung function. Recently, it was demonstrated that hepatocyte growth factor receptor (c-Met) expression is required for neutrophils' extravasation to inflamed tumors, through inflammatory stimuli. Accordingly, we hypothesized that inflammatory cells recruitment, as neutrophils, is attenuated during pulmonary fibrosis in mice with *c-Met*-deleted immune cells, with subsequent decline of fibrosis progression and lung function preservation. In this way, the purpose of this thesis was to understand the role of c-Met expression in immune cells in the pathogenesis of pulmonary fibrosis and associated-inflammation. To answer this, bleomycin (BLM)-induced lung fibrosis model was used in *c-Met*$^{fl/fl}$/Tie2:Cre-positive transgenic (TG) mice, in which *c-Met*-floxed gene is excised from hematopoietic and endothelial cells.

Survival analysis was performed until day 21 after BLM administration, in which TG mice exhibited increased survival and less weight loss compared to wild-type (WT). Next, lung fibrosis extent was determined 14 days after administration on Masson's trichrome stained lung sections. TG mice presented significantly reduced fibrotic score, characterized by reduced alveolar destruction and extracellular matrix deposition. Moreover, using hydroxyproline assay, collagen levels were diminished in TG mice lungs, in accordance with the significant decrease of collagen (*Col1a1 and Col1a2*), as well as a fibroblast marker (*S100a4*) and a profibrotic factor (*Igf-1*) transcript' levels. At day 7 after administration, tissue cytotoxicity, assessed by lactate dehydrogenase assay, was reduced in TG mice. This comes in agreement with reduction of inflammatory cells recruitment, specifically neutrophils and inflammatory macrophages, evaluated by flow cytometry. Moreover, TG mice presented an increase in transcript' levels of proinflammatory cytokines (*Tnf-α, IL-1β, IL-6* and *iNos*).

Taken together, our findings propose that *c-Met* deletion in immune cells attenuates pulmonary fibrosis progression, probably due to reduction of inflammatory cells, specifically neutrophils and inflammatory macrophages, in injured lung and consequent decrease in the production of profibrotic factors, as Igf-1.

# Resumo

A fibrose pulmonar idiopática (IPF) é uma doença pulmonar debilitante e rápida, sendo a forma mais comum e letal de doenças pulmonares intersticiais, cujas causas permanecem desconhecidas. Atualmente, não há terapia médica capaz de reverter a progressão da doença. Esta doença compreende uma inflamação crónica, na qual as proteases derivadas de neutrófilos foram descritas como mediadores chave do dano tecidular e, consequentemente, declínio da função pulmonar. Recentemente, foi demonstrado que a expressão do recetor do fator de crescimento de hepatócitos (c-Met) é necessária para o extravasamento de neutrófilos para tumores inflamados, aquando dos estímulos inflamatórios. Nesse sentido, hipotetizamos que o recrutamento de células inflamatórias, como neutrófilos, está atenuado durante a fibrose pulmonar em ratinhos com deleção de *c-Met* em células hematopoiéticas e endoteliais, com subsequente diminuição do processo fibrótico e função pulmonar preservada. Desta forma, o objetivo desta tese foi compreender o papel da expressão de c-Met em células imunes na patogénese da fibrose pulmonar e inflamação associada. Para responder a isso, o modelo de fibrose pulmonar induzido por bleomicina (BLM) foi usado em ratinhos transgénicos (TG) *c-Met*$^{fl/fl}$/Tie2:Cre-positiva, nos quais o gene *c-Met* é deletado em células hematopoiéticas e endoteliais.

A análise de sobrevivência foi realizada até ao dia 21 após a administração de BLM, os ratinhos TG exibiram maior sobrevivência e menor perda de peso em comparação com o tipo selvagem (WT). Em seguida, a extensão da fibrose pulmonar foi determinada 14 dias após a administração, em secções de pulmão coradas com tricrómio de Masson. Os ratinhos TG apresentaram classificação fibrótica pulmonar significativamente reduzida, caracterizados pela redução da destruição alveolar e deposição de matriz extracelular. Além disso, utilizando o ensaio de hidroxiprolina, os níveis de colagénio estavam reduzidos em ratinhos TG, o que vem de acordo com a diminuição significativa dos níveis de transcritos de colágeno (*Col1a1* e *Col1a2*), bem como de um marcador de fibroblastos (*S100a4*) e um fator pró-fibrótico (*Igf-1*). No dia 7 após a administração, a citotoxicidade do tecido, avaliada pelo ensaio da lactato desidrogenase, estava reduzida nos ratinhos TG. Isto está de acordo com a redução do recrutamento de células inflamatórias, especificamente neutrófilos e macrófagos inflamatórios, avaliados por citometria de fluxo. Além disso, os ratinhos TG apresentaram um aumento nos níveis de transcritos de citocinas pró-inflamatórias (*Tnf-α, IL-1β, IL-6, iNos*).

Em conjunto, os nossos resultados sugerem que a deleção de *c-Met* em células imunes atenua a progressão da fibrose pulmonar, provavelmente devido à redução de células inflamatórias,

especificamente neutrófilos e macrófagos inflamatórios, no pulmão lesionado e consequente diminuição da produção de fatores pró-fibróticos, como o Igf-1.

# Table of Contents

# List of Abbreviations

**A**

**ACK-** Ammonium-chloride-potassium

**AEC-** Alveolar epithelial cells

**AKT-** Protein kinase B

**AM-** Alveolar macrophage

**α-SMA-** Alpha-smooth muscle actin

**B**

**BAL-** Bronchoalveolar lavage

**BALF-** BAL fluid

**BLM-** Bleomycin

**bp-** Base pair

**BV-** Brilliant violet

**C**

**Col-** Collagen

**CT-** Threshold cycle

**CTGF-** Connective tissue growth factor

**D**

**DAPI-** 4′,6-diamidino-2-phenylindole

**DMEM-** Dulbecco's modified eagle medium

**E**

**EC-** Epithelial cells

**ECM-** Extracellular matrix

**F**

**FACS-** Fluorescence-activated cell sorting

**FAK-** Focal adhesion kinase

**FBS-** Fetal bovine serum

**FSC-** Forward scatter

**G**

**Gapdh-** Gliceraldehyde-3-phosphate dehydrogenase

**H**

**H&E-** Hematoxylin and eosin

**HGF-** Hepatocyte growth factor

**HP-** Hydroxyproline

**HRCT-** High resolution computed tomography

**I**

**IL-** Interleukin

**IM-** Interstitial macrophage

**iNOS-** Inducible nitric oxide synthase

**IPF-** Idiopathic pulmonary fibrosis

**IT-** Intratracheal(ly)

**L**

**Ly-6C-** Lymphocyte antigen 6 complex locus C

**Ly-6G-** Lymphocyte antigen 6 complex locus G

**M**

**MIP-** Macrophage inflammatory protein

**MMP-** Metalloproteinases

**mRNA-** Messenger RNA

**M1-** Classically activated macrophages

**M2-** Alternatively activated macrophages

**N**

**NAC-** N-acetylcysteine

**NE-** Neutrophil elastase

**P**

**PBS-** Phosphate-buffered saline

**PCR-** Polymerase chain reaction

**PFA-** Paraformaldehyde

**PI3K-** Phosphoinositide-3 kinase

**R**

**ROS-** Reactive oxygen species

**RT-** Room temperature

**RT-qPCR-** Reverse transcriptase-quantitative polymerase chain reaction

**S**

**SSC-** Side scatter

**STAT-** Signal transducer and activator of transcription

**T**

**TG-** Transgenic

**TGF-β-** Transforming growth factor-beta

**TIMP-** Tissue inhibitors of metalloproteinases

**TNF-α-** Tumor necrosis factor-alpha

**U**

**UIP-** Usual interstitial pneumonia

**W**

**WT-** Wild-type

# List of Figures

# List of Tables

CHAPTER 1

# INTRODUCTION

# 1. Introduction

Fibrosis is a pathologic feature of most chronic lung diseases, such as interstitial lung disease (ILD) and idiopathic interstitial pneumonias. Generally occurs as result from a variety of lung insults, including auto-immune, drug-induced, infectious and traumatic injuries [1, 2].

## 1.1 Idiopathic pulmonary fibrosis

Idiopathic pulmonary fibrosis (IPF) is the most common type of ILD, which causes remain unknown. Furthermore, IPF is a lethal specific form of chronic, progressive fibrosing interstitial pneumonia affecting mainly middle-aged and elderly males, with an increasingly incidence all over the world. IPF affects 3 million people worldwide, these number was estimated by Martinez *et al.* as the population prevalence is 130,000 in the United States, 300,000 in Europe and 640,000 in East Asia [3].

Although the causes of this disease are still under investigation, some risk factors are already associated with an increased incidence of the disease, namely genetic predisposition, advanced age, male gender, gastroesophageal reflux, tobacco smoking, microbial infections and exposure to therapeutic or environmental toxins [4].

Some studies suggest that mortality rate exceeds that of several types of cancers which affect people with similar demographics, except lung and pancreatic cancer [5,6] (Figure 1). Importantly, survival is relatively variable between patients [7], with a median survival of 3–5 years from diagnosis [4].

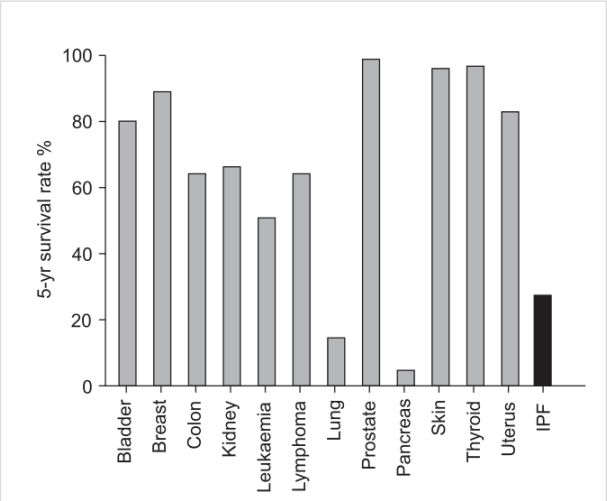


**Figure 1: Comparison of the 5-year survival rate of IPF and different types of cancer with similar demographics (USA).** 20% to 40% of IPF patients survive for more than 5 years. Vancheri *et al.* 2010 [6].

### 1.1.1 Diagnosis and Therapy

IPF is suspected when adult patients present unexplained exertional dyspnoea, cough, bibasilar inspiratory crackles and finger clubbing. These patients should be carefully evaluated for exclusion of other known causes of ILD, as for example risk exposures, immunologic profile and lymphocytosis [8] (Figure 2). The next diagnostic approach is high resolution computed tomography (HRCT), that provides detailed imaging of lung parenchyma, by which three categories can be detected, usual interstitial pneumonia (UIP), possible UIP and inconsistent with UIP pattern [4,9,10].

According to current American Thoracic Society/European Respiratory Society/Japanese Respiratory Society/Latin American Thoracic Society guidelines the presence of a reliable UIP pattern in the right clinical setting and the absence of alternative diagnoses, provide a definite IPF diagnosis [4,9,10]. These patients present radiologic and/or histopathologic patterns consistent with UIP as described in the 2002 statement [11], including basal-predominant reticular abnormality, 'honey-combing', consisting in subpleural cystic airspaces with well-defined walls, with or without traction bronchiectasis (dilatation of the bronchi) and peripheral alveolar septal thickening [3].

In case of a possible UIP pattern (i.e. same pattern, however no honeycombing) a surgical lung biopsy is recommended, which frequently is impractical because of disease severity, possible aggravation and comorbidities [4,9].

Multidisciplinary discussion among different experts (including pulmonologists, radiologists, pathologists and thoracic surgeons in selected cases) has demonstrated to improve diagnostic accuracy, specially recommended before the final diagnosis or in case of discordant radiologic and histopathologic patterns (e.g., HRCT is inconsistent with UIP and histopathology consist with UIP) [4].

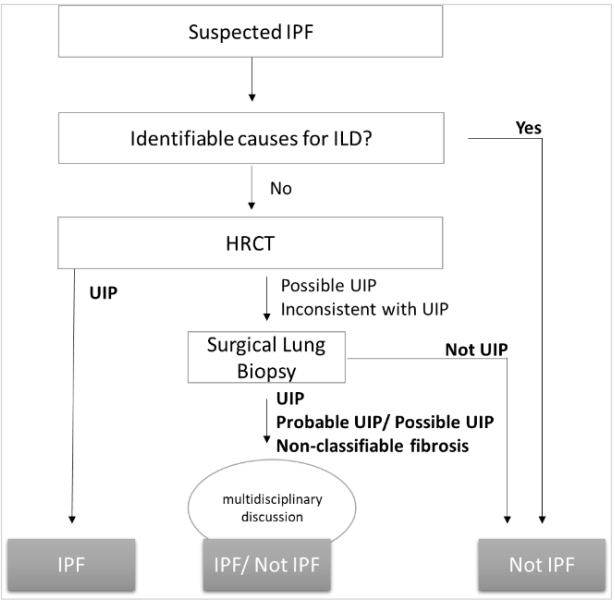


**Figure 2: IPF diagnostic algorithm.**

Patients with suspected IPF should be carefully evaluated for identifiable causes of other ILD. The absence of identifiable cause for other ILD and HRCT clearly indicating UIP pattern is enough to IPF diagnosis. In the absence of consistent UIP pattern on HRCT, IPF can be diagnosed by the combination HRCT and histopathological patterns. The accuracy of the diagnosis of IPF increases with multidisciplinary discussion among ILD experts. Adapted from Raghu *et al.* 2011 [4].

Currently, there is no medical therapy capable of revert disease progression. Therapeutic strategy traditionally used for IPF consisted in the combination of corticosteroids (prednisone) with azathioprine and N-acetylcysteine (NAC), since it was believed that uncontrolled chronic inflammation was the main driver of progressive parenchymal fibrosis. However, unfortunately a clinical trial found increased risk of death and hospitalization in patients under this treatment regimen, particularly popular in Europe during several years [12]. After numerous therapeutic efforts with ineffective results, in 2014 two promising drugs emerged, pirfenidone and nintedanib (Table 1). Pirfenidone is a pleiotropic molecule orally available with versatile antifibrotic effects, capable of attenuating transforming growth factor (TGF)-β-mediated pathways, as so supressing fibrogenic activity of human lung fibroblast [13,14]. On the other hand, nintedanib is an intracellular inhibitor that targets multiple tyrosine kinases, including the receptors of vascular endothelial growth factor, fibroblast growth factor and platelet-derived growth factor [15]. More recently, lung transplantation has emerged as a promising strategy, with 50% chance survival rate 5 years after transplantation [16]. As a complement and when transplantation is ineligible, nintedanib and pirfenidone are capable of partially slow fibrotic progression but neither are curative or even regressive [15,13]. In this way, effective methods for prevention and treatment of pulmonary fibrosis (PF) are needed.

**Table 1: Pharmacologic management of IPF.**

IPF affects millions of individuals worldwide faced with lack of available therapies capable of reversing disease progression. Lederer *et al.* 2018 [17].

| Agent/Therapy | Potential mechanism of action | Effect | Recommendation |
|---|---|---|---|
| Combined prednisone, azathioprine and NAC | Anti-inflammatory, cytotoxic and anti-oxidant | - | Strong recommendation against use |
| NAC monotherapy | Anti-oxidant | - | Conditional recommendation against use |
| Nintedanib | Tyrosine kinases intracellular inhibition<br>Targets multiple growth factor receptors, including vascular endothelial growth factor, fibroblast growth factor, and PDGF | Slows forced vital capacity decline by 50% | Conditional recommendation for use |
| Pirfenidone | Antifibrotic drug with pleiotropic effect, direct mechanism unknown<br>In animal models leads to inhibition of TGF-β production and downstream signaling, collagen synthesis, and fibroblast proliferation | Slows forced vital capacity decline by 50% | Conditional recommendation for use |

Despite some new findings, the lack of understanding of etiology and pathogenesis make it a life-threatening disease. The unpredictability and heterogeneity of disease behaviour, probably due to the wide range of mediators, growth factors and signaling pathways behind the fibrotic process [18], represent the main difficulties when choosing the appropriate outcome measurements to be monitored and the design of clinical trials. Undoubtedly, new insights into disease pathogenesis will allow the identification of novel therapeutic targets, culminating in more efficient compounds to prevent and restrain all stages of this disease.

### 1.1.2 Pathogenesis

ILD share the propensity for PF and among these diffuse parenchymal lung disorders we can find IPF, sarcoidosis, as well as collagen vascular diseases, such as rheumatoid arthritis and scleroderma [19], being among them IPF the most common and lethal form. This disease is histologically characterized by scattered fibroblastic foci, clusters of active local fibroblasts proliferation, in the background of dense acellular collagen. This scarring and thickening of the interstitium, the space between the vascular endothelium and the alveolar epithelium, is due to the progressive deposition extracellular matrix (ECM) and collagen, resulting in architectural distortion and alveolar collapse [20]. These changes, amongst other possible complications, difficult oxygen exchange and the lung expansion becomes tougher, leading to breathlessness and consequently death [21].

For many years, IPF was considered a principally sporadic chronic interstitial inflammatory process. However, current experimental evidences have shifted the disease paradigm (Figure 3). It has been demonstrated that aberrant activation of injured alveolar epithelial cells (AEC), mainly AEC type 2, leads to the cross-talk between debilitated AEC and the nearby mesenchymal compartment resulting in abnormal or persistent activation of tissue repair pathways [20] (Figure 3A). AEC have been described to be responsible for the production of mediators that induce the formation of fibroblastic foci, influx of circulating fibrocytes and stimulation of the epithelial-mesenchymal transition. During this process, epithelial cells lose the expression of epithelial adhesion molecules, E-cadherin, gaining mesenchymal adhesion protein N-cadherin and mesenchymal markers such as fibronectin, vimentin and fibroblast specific protein-1 (also known as S100a4) and acquire migratory capacity [22,23].

Recently increasing importance has been attributed to the inflammatory component in the disease progression, namely involved cells and signaling. Detailed description of evidences of this close involvement will be mentioned in the next section. Initially, a stimulus leads to AEC injury, which generates mediators and apoptotic cells, culminating in the recruitment and activation of several immune cells including macrophages, neutrophils and lymphocytes that produce several cytokines (Figure 3B). The origin of the insult or causative agent determines the character of the resultant inflammatory response and drastically influences resident tissue cells [24], in case of taking uncontrolled proportions this process can contribute to cellular damage and tissue destruction. As shown in Figure 3B these inflammatory cells and the secreted mediators induce the activation of fibroblasts and consequently excessive deposition of ECM.

In these processes, aberrant activation and proliferation of interstitial and recruit fibroblasts and their differentiation into active myofibroblasts [25], is responsible for the excessive production and deposition of interstitial matrix [26,27] (Figure 3C). Myofibroblast present a contractile phenotype that is characterized by features of fibroblasts and presence of α-smooth muscle (α-SMA) stress fibers and secrete excessive amounts of collagen and ECM proteins [28]. This uncontrolled process leads to architectural distortion, loss of lung elasticity and alveolar surface area, consequently occurring an impairment of gas exchange and irreversible loss of function [18].

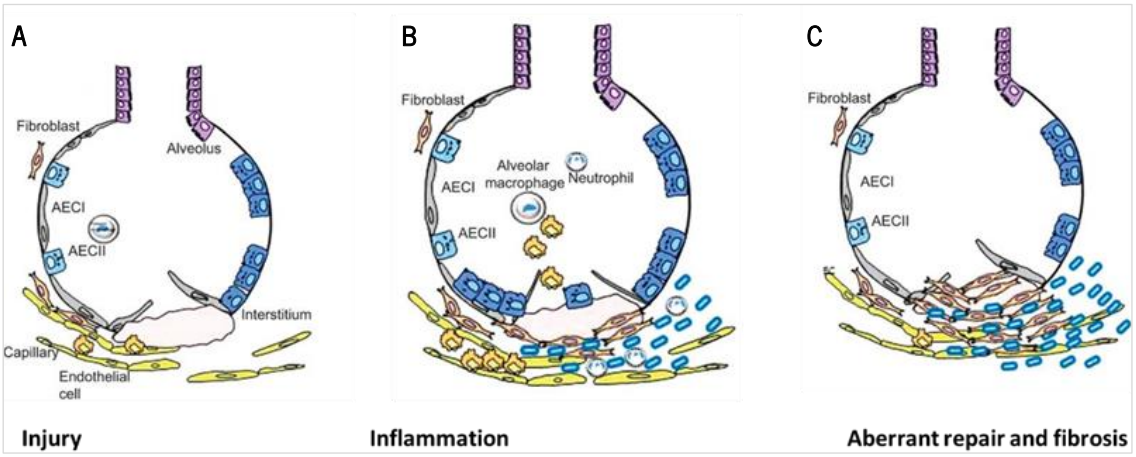


**Figure 3: IPF pathogenesis.**

Main characteristic features of IPF progression. (A) Multiple or persistent injuries lead to AEC apoptosis and phenotypic alterations. The early phase after tissue injury is characterized by increased innate immune system activation by dead or dying cells. (B) Uncontrolled tissue damage could trigger an adverse chronic inflammation. (C) Wound healing is characterized by activation and differentiation of fibroblast into myofibroblasts driving abnormal production of ECM, which ultimately lead to architectural distortion and loss of function. Adapted from Wuyts, W. *et al.* 2013 [29].

Although the mechanisms and mediators involving epithelial cell dysfunction and fibrosis have not yet been fully understood, the crosstalk between epithelial cells, the ECM, adjacent mesenchymal and inflammatory populations is clearly fundamental to this process.

Following AEC injury, several signaling pathways must be carefully balanced to enable effective and functional repair. The injured epithelium and recruited inflammatory cells can modulate epithelial repair, promote fibroblast recruitment and myofibroblast activation by secretion of several mediators (Figure 4). IPF patients recurrently present a profibrotic cytokines and growth factors profile, namely interleukin (IL)-1β, tumor necrosis factor (TNF)-α, TGF-β and platelet-derived growth factors (PDGF) [30], being TGF-β1 the most potent factor known to promote fibrotic diseases [31,32]. Although this factor is produced and targets several cell types, Tgf-β1 isoform predominantly derives from circulating monocytes and tissue macrophages, which once active acts in fibrogenic cells, namely in fibroblasts stimulating proliferation and differentiation into myofibroblasts, which are able to secrete Tgf-β and synthetize ECM proteins [31,33,34]. Connective tissue growth factor (Ctgf), is another important fibrogenic factor, considered a downstream mediator of Tgf-β1 responses [35,36], being capable of induce α-SMA expression reflecting fibroblasts differentiation into myofibroblasts [37]. Besides Tgf-β and Ctgf, Pdgf also promotes pulmonary fibrosis through fibroblast activation [38] and it is a potent chemoattractant for inflammatory cells [39]. Furthermore, the lung of IPF patients present increased PDGF expression in epithelial cells and macrophages [40] and its *in vivo* overexpression lead to severe pulmonary fibrosis [41]. Imatinib, a PDGF

tyrosine kinase inhibitor, presented strong antifibrotic effects in bleomycin (BLM)-induced pulmonary fibrosis through inhibition of mesenchymal cell proliferation [42]. However in IPF patients it presents neither a survival benefit nor amelioration in respiratory capacity [43]. IL-1β, a proinflammatory cytokine, contributes to the fibrotic disease progression [44], also exacerbates parenchymal-cell injury [39]. Furthermore, blockade of Tnf-α, IL-1, IL-6 or Tgf-β can reduce inflammation and resultant fibrotic response following BLM administration [45,46,47,48].

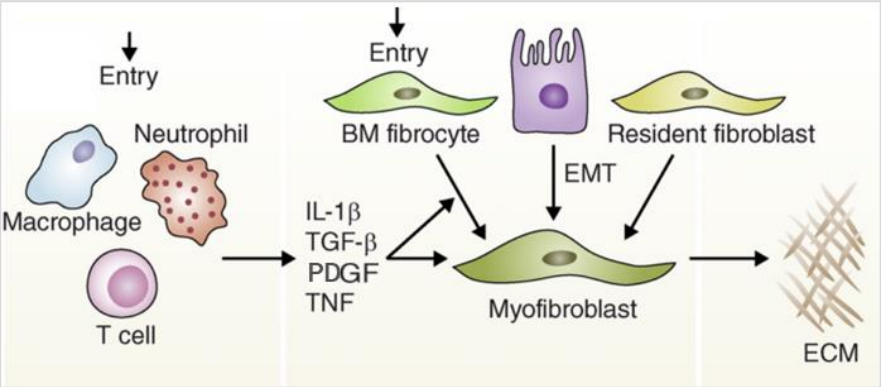


**Figure 4: Proinflammatory and profibrotic mediators in the maintenance of fibrosis.**

After lung injury, epithelial cells release inflammatory mediators followed by influx of leukocytes (e.g., neutrophils, macrophages and T cells). The recruited leukocytes secrete profibrotic cytokines such as IL-1β, TGF-β, PDGF and TNF. The activated macrophages and neutrophils remove dead cells and eliminate any invading organisms. In the subsequent phase, fibrocytes from the bone marrow and resident fibroblasts proliferate and differentiate into myofibroblasts, which release ECM components. Adapted from Wynn 2011 [49].

### 1.1.3 Inflammatory reaction during disease progression

Inflammation during fibrosis has a double-edged function that will be detailed below, however the most well-understood role and known mediators are those that directly act in simultaneous to the fibrogenic process. As shown in Figure 3, an initial acute inflammatory recruitment is induced and appears to promote fibrosis. In contrast a late inflammatory reaction prevents the profibrotic outcome [24]. Once both inflammatory onsets are essential for this purpose, there is a need to better understand the inflammatory mechanisms involved in the disease progression. Several studies described that inflammatory reaction is capable of triggering the pulmonary fibrosis initiation [50,51]. In this way persistent or unresolved tissue inflammatory response can lead to injury of resident epithelial cells. Furthermore, chronic inflammation can result in enhanced release of inflammatory mediators, which in turn activate effector cells, driving the pulmonary fibrosis progression [25,52].

In the early-stage of BLM-induced lung fibrosis the accumulation of neutrophils [53] and macrophages [54] has been described as an important event for the transition from inflammatory to

fibrotic process. Similar studies in IPF patients showing that various inflammatory cells can be found in the lung of patients, including macrophages, neutrophils and lymphocytes, several animal models of fibrotic diseases demonstrate a role for the referred inflammatory cells, likewise their secreted cytokines, chemokine and proteases [55]. Furthermore, the inflammatory influx in human lung biopsies correlates with a worse prognosis [56], also suggesting a significant role for these cells in disease progression.

Neutrophils are innate immune cells, with rapid and potent phagocytic capacity, not just antibacterial effectors [55,57], but also capable of shaping their tissue environment by releasing proteases and oxidants [57,58,59,60]. In the 1980's neutrophils were described as crucial contributors to the lung pathology, once bronchoalveolar lavage (BALF) of IPF patients present high levels of activated neutrophils [61]. The accumulation of these cells in IPF patients' BALF predicts earlier mortality [62], likewise when these cells infiltrate within honeycombed areas, patients present an early mortality [63,64]. Moreover, their infiltration characterizes the alveolitis inherent to IPF, accompanied with high levels of neutrophil elastase (NE) within lung parenchyma [65], which induces both fibroblast proliferation and myofibroblast differentiation *in vitro* [66]. Neutrophils produce several proteases, such as matrix metalloproteinase (MMP), that degrade ECM components. In contrary, these cells have the ability to enhance ECM deposition through the production of NE and tissue inhibitors of metalloproteinases (TIMP) [55]. In addition, Sivelestat and ONO-5046•Na, NE inhibitors attenuated BLM-induced pulmonary fibrosis in mice, the first inhibitor is described to act via suppression of Tgf-β1 activation and inflammatory cell recruitment to the lungs [58,59].

More recently, macrophages and associated cytokines have been demonstrated to be important and currently research is mainly focused on the mononuclear phagocytes [50].

Macrophages can contribute to wound repair after tissue injury, through their capacity of scavenger cells, phagocytizing cellular debris, invading organisms, neutrophils and other apoptotic cells. Pulmonary macrophage populations divide into alveolar macrophages (AM), located in the airways and expressing high expression of Siglec F, with CD11b expression or not, and interstitial macrophages (IM), placed within the lung parenchyma and express high levels of CD11b and lack of Siglec F expression [67]. Maintenance of immunologic homeostasis and host defence in the lung are assured by AMs, exerting their regulatory effects via non-specific lines of defence, as high phagocytic ability, secretion of nitric oxide, Tnf-α and Ifn-γ [68]. While IMs are believed to have a regulatory role within the lung tissue, associated with greater tendency to release cytokines related with the adaptive immune response, such as IL-10 [68].

Recent studies established distinct roles for macrophages during the inflammatory and recovery phases of wound healing and fibrosis. Indeed, early macrophages depletion after injury often greatly diminished the inflammatory response. In this way a study in liver fibrosis using CD11b-diphtheria toxin receptor mice described that macrophages depletion during the early inflammatory phase lead to reduced scarring and fewer myofibroblasts. In contrast, if macrophages were depleted during the late recovery phase, fibrosis persisted [69]. A similar study targeted CD11b cells by means of antibodies in silica and BLM animal models showing that the inhibition of these cells extravasation lead to a dramatic reduction of pulmonary collagen and fibrosis [70].

Macrophages represent a potent source of chemokines and other mediators that drive the initial cellular response following injury, as secretion of the inflammatory cytokine Tnf-α, IL-1β, IL-6 [71,72]. After the early inflammation-associated fibrosis phase decline, the predominant macrophage population assumes a wound-healing phenotype that is characterized by the production of numerous growth factors, including Pdgf, Tgf-β1, insulin-like growth factor-1 (Igf-1), and vascular endothelial growth factor-α, which promote cellular proliferation and blood-vessel development [71,72].

Local tissue microenvironment, namely released growth factors and cytokines, modulates the recruited and resident macrophages proliferation, phenotype and function. Particularly, macrophages demonstrate remarkable diversity and plasticity, being capable of assume different phenotypes which can both drive or resolve fibroproliferative responses to injury. Contrasting macrophage phenotypes, M1 (classically activated) and M2 (alternatively activated), are keys to understanding the beneficial versus harmful roles of macrophages in fibrotic diseases. These cells can be categorized in two main groups: M1-like known to be involved in the production of ECM degrading MMP, proinflammatory cytokines and myofibroblasts apoptosis during disease, identified by its proinflammatory behavior and the synthesis of inducible nitric oxide synthase (iNos), IL-1β and Tnf-α; and M2-like macrophages are implicated in the aberrant wound-healing cascade during fibrosis because of their production of tissue inhibitor of metalloproteinases and profibrotic cytokines, such as IL-4, Tgf-β and IL-10 [55, 68]

Additionally, T cells participate in pulmonary host defence against bacterial, viral and fungal pathogens, and can be divided in CD8+ (cytotoxic T cells) and CD4+ (helper T cells) which help B cells to mount antibody responses, enhance and maintain responses of cytotoxic T cells. Moreover, two distinct populations of CD4+ T cells were then designated as T helper (Th)1 and Th2 cells, distinguished mainly by the effector cytokines they produce but also by their expression of different

patterns of cell surface molecules and transcription factors mentioned below. Inconsistent results have been described for lymphocytes' role in fibrosis, namely some suggest that lymphocytes in honeycombed areas of the lung predict an increased survival and these lymphocytes present elevated ratio CD4/CD8 T-cells [73,63], pointing up the importance of this subpopulation in the disease attenuation. In contrast a study in BLM-induced pulmonary fibrosis using anti-CD3 monoclonal antibody showed that systemic depletion of T cells reduces ECM accumulation and fibrosis [74]. Interestingly, Th-1 and Th-2 cells have been associated with IPF pathogenesis and have opposing roles. The Th1 cytokines, interferon (IFN)-γ and IL-12 attenuated fibrosis [75], while the typical Th2 cytokines, IL-4 and IL-13 have been shown to stimulate fibroblast proliferation, differentiation into myofibroblasts and collagen production [76,77], establishing the notion that Th1 responses are antifibrotic, protective, whereas Th2 responses are profibrotic, harmful [78,49,77]. The known effects described for both adaptive and innate immune cells are outlined in the Figure 5.

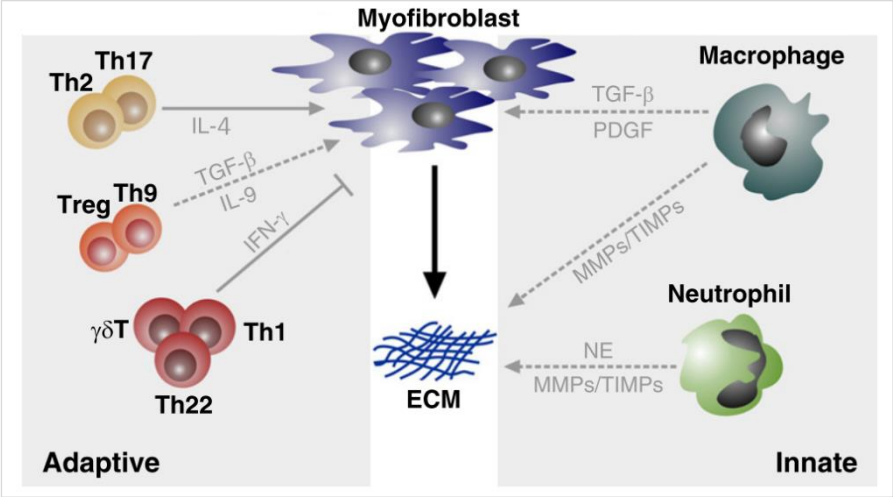


**Figure 5: Effect of immune cells on myofibroblasts and fibrosis progression.**

Impact of components from the innate (macrophages and neutrophils) and adaptive (T cells) immune system in fibrosis progression. Cytokines, growth factors and enzymes released directly promote fibroblast activation and lead to myofibroblast activation via further induction of proinflammatory, profibrotic factors in other immune cells. Adapted from Kolahian *et al.* 2016 [55].

Recent studies have introduced the role of a bone marrow-derived mesenchymal progenitor cells, the fibrocytes, which are capable to extravasate into wounded tissue and differentiate into fibroblasts and myofibroblasts [79,80]. Fibrocytes are circulating myeloid-derived cells that are characterized by their surface phenotype, expressing hematopoietic (CD45, CD34) and mesenchymal (type I collagen) cell markers, corresponding to a hematopoietic progenitor, with fibroblast-like phenotype [81]. Additionally, fibrocytes secrete paracrine factors, activating resident fibroblasts which promote lung fibrosis [82]. Interestingly, IPF patients present elevated circulating

fibrocytes, as so being considered a prognostic marker and a predictor of poor survival [83]. The role of fibrocytes in lung fibrosis has been described using BLM-induced lung injury, where inhibiting their migration to the lung lead to attenuated pulmonary fibrosis [84].

## 1.2 Mouse models of pulmonary fibrosis

Animal models play a crucial role for the study of human diseases and many models are established to understand their pathogenesis, respective predictors and new therapeutic approaches. Although different models of pulmonary fibrosis have been developed, none of them fully mimic human IPF. However, the use of animal models is indispensable for research progression, further prognostic examinations and therapies [8,85].

The known animal models of fibrosis allowed the identification of new insights into the pathobiology of lung injury, inflammation and fibroproliferation [85], namely many key cells, involved processes and mediators in human lung fibrosis. These models include radiation; instillation of BLM, silica or asbestos; transgenic mice or gene transfer employing fibrogenic cytokines. So far, the most used model for induction of experimental pulmonary fibrosis in rodents is BLM. The main features, advantages, and disadvantages of the mentioned models are summarized in Table 2.

**Table 2: Feature, advantages and disadvantages of fibrosis animal models.**
Adapted from Moore *et al.* 2008 [85] and Moore *et al.* 2013 [86].

| Model | Features | Advantages | Disadvantages |
|---|---|---|---|
| **Bleomycin** | Cell injury<br>AEC hyperproliferation<br>Acute model | Well-established<br>Reproducible<br>Clinical relevance<br>Short time frame (14-28 days)<br>Multiple routes of delivery | Expensive<br>Reversible effects 28 days after single injection |
| **Radiation** | AEC damage<br>Vascular remodelling<br>Mesenchymal stem cells regulate repair responses | Clinical relevance | Long time frame (>30 wk)<br>Expensive<br>Strain-dependent effects |
| **Inhaled irritants (Silica/Asbestos/ Cigarette smoke)** | AEC damage<br>Fibroblastic foci<br>Macrophage oxidative stress<br>Chronic model | Fibrotic nodules resemble those seen in humans<br>Persistent fibrosis | Long time frame (12-16 wk)<br>Difficult delivery<br>Lack of reproducibility<br>Absence of UIP-like lesions<br>Strain-dependent effects |
| **Transgenic** | Understanding signaling events related to specific fibrotic-inducing molecules | Allow to study overexpression of specific molecules<br>Capable of being expressed under inducible promoters even only in adult life | Compensations may occur in mice that constitutively express a transgene throughout development<br>Amount of product produced may not be physiological<br>Limited to specific pathways |

### 1.2.1 The bleomycin animal model

BLM, produced by the bacterium "*Streptomyces verticillus*", is one of the first described chemotherapeutic agent [87] and played an important role in the treatment of lymphoma, squamous cell carcinomas, germ cell tumors and malignant pleural effusion [88]. Lung injury and subsequent pulmonary fibrosis upon long-term BLM administration was found to be one of the adverse drug effects in human cancer therapy, being the reason why it began to be used as inducer of lung fibrosis in animal models [88].

BLM hydrolase, is an enzyme capable of metabolize BLM, as so influencing the effects of this drug on many tissues. Remarkably, the lungs and the skin are the most common sites of BLM toxicity which keep low levels of this hydrolase, thus having higher susceptibility to tissue injury [87].

BLM-induced pulmonary fibrosis is extensively accepted as murine model of IPF. Currently, it is believed that it induces single and double-strand DNA breaks in cells, interrupting the cell cycle. This is the effect of metal ions chelation, forming a pseudoenzyme which reacts with oxygen, resulting in the production of DNA adducts and excess DNA-cleaving superoxide and hydroxide free radicals [89]. Subsequently reactive oxygen species (ROS) overproduced mediate lipid peroxidation and protein oxidation, which can trigger an inflammatory process, leading to pulmonary toxicity, activation of fibroblasts and lastly fibrosis [90,91].

Single intratracheal (IT) BLM administration causes inflammatory and fibrotic processes within a short period of time (Figure 6). In this model, an acute inflammatory reaction is dominant during the first week after administration, along with an initial elevation of proinflammatory cytokines (IL-1, Tnf-α, IL-6, Ifn-γ). Thereafter the inflammatory reaction disappears gradually, the "switch" between inflammation and fibrosis appears to occur around day 9 after BLM administration [90], and by day 14 the peak of fibrogenic changes can be detected biochemically and histologically. These fibrogenic changes include fibroblasts proliferation and ECM deposition, accompanied by increased expression of profibrotic markers (Tgf-β1, fibronectin, procollagen-1), with maximal responses generally noted around days 21–28 [85,92,88].

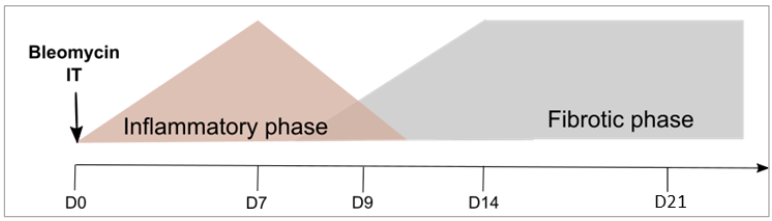


**Figure 6: Temporal progression of BLM-induced pulmonary fibrosis in mice.**

After administration of BLM, an acute inflammatory reaction lasting up to a week, is followed by fibrogenic processes, with a peak by day 14, leading to matrix deposition and impaired lung structure out to 21 days.

Notable the major advantages of BLM model are the relatively easy performance, wide accessibility and reproducibility and the fulfilment of relevant criteria expected from a good animal model. As mentioned, BLM triggers the overproduction of ROS, causing an inflammatory response with induction of proinflammatory cytokines and activation of macrophages and neutrophils, thus resembling these acute lung injury aspects [88]. However, in the final stage this model present the disadvantage of being at least partially reversible, so does not recapitulate the concept irreversible feature of IPF in patients [93,94].

## 1.3 Hepatocyte growth factor/c-Met signaling pathway

Hepatocyte growth factor (HGF) is a multifunctional growth factor, with a broad activity and has impact on many physiologic and pathologic processes. These effects are mediated by its specific cell-surface receptor, the proto-oncogenic c-Met, a heterodimeric tyrosine kinase with a single transmembrane region and a conserved tyrosine kinase domain [95] (Figure 7). It can induce cellular motility, survival, proliferation or morphogenesis depending upon the target organ and cell type [96].

Recently, importance of c-Met have increasingly been focused due to its close involvement in cancer [97]. Regarding this topic, HGF has been described to play critical roles in proliferation, migration, invasion, tumor angiogenesis and lymph angiogenesis [95]. Besides this close association with cancer, c-Met has been described in other pathologic conditions such as lung related diseases. In different injury and disease models, mentioned in the following subsection, HGF promotes cell survival, regeneration of tissues, suppresses chronic inflammation and improves fibrosis.

As mentioned besides cancer, tissue injury leads to pro-HGF proteolytic activation, the binding from the active form to the c-Met receptor induces activation of tyrosine kinase and the auto-phosphorylation of two critical tyrosine residues in c-Met [98]. Multiple signal transduction pathways can be activated by HGF/c-Met signaling, among the many important signaling cascades are the Src/focal adhesion kinase (FAK) pathway, the p120/signal transducer and activator of transcription (STAT) 3 pathway, the phosphoinositide-3 kinase (PI3K)/Akt pathway and the Ras/MEK/ERK pathway [99,100,101] (Figure 7).

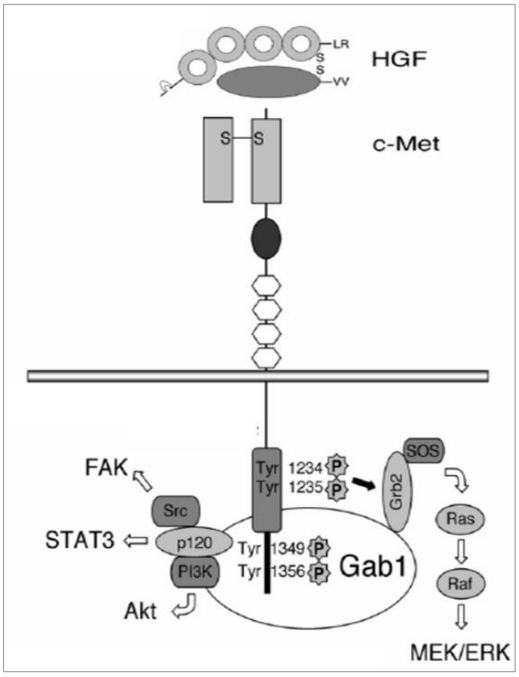


**Figure 7: Summary of the HGF/c-Met signaling pathways.**

HGF/c-Met signal transduction is initiated by binding of HGF to c-Met. Dimerization c-Met activates phosphorylation of tyrosines (Tyr1234 and Tyr 1235) in the kinase domain followed by additional phosphorylation of other tyrosines (Tyr 1349 and Tyr 1356) in the C-terminal regulatory tail. Fully activated c-Met propagates HGF signaling in cells by recruiting and activating various adapter molecules downstream. Weon-Kyoo You *et al.* 2008 [101].

### 1.3.1 HGF/c-Met signaling in lung homeostasis, injury and repair

In lung development HGF/c-Met is required to coordinate epithelial and vascular development. During development HGF is produced in endothelial cells and HGF/c-Met signaling acts in respiratory epithelium for normal septae formation [102].

In normal conditions c-Met is expressed both in endothelial cells and alveolar epithelial cells, however once the signaling is not activated, it plays no role during homeostatic conditions [103].

After lung injury, this signaling acts in c-Met expressing AEC2 being responsible for their proliferation and preventing apoptosis [103,104,105] and in myofibroblasts, in this case c-Met expression is induced by Tgf-β1, enhancing apoptosis and ECM degradation [106,107]. During emphysema HGF acts in lung vascular endothelial cells promoting alveolar angiogenesis [108].

Recently, increasing interest is attributed to the role of HGF in lung repair. In mouse lung recombinant human HGF contributes to lung repair process that follows BLM-induced lung injury in murine models, as critical inducer of AEC proliferation [109] and myofibroblast apoptosis [107] along with ECM degradation [106], followed by improvement in clinical findings. In the same way, using different animal models of lung injury, administration of exogenous HGF promotes lung repair and

reduces fibrosis [110]. Notably, HGF protective effects are potentiated when given in simultaneous with or 7 days after the administration of a profibrotic agent [106,111]. These findings reveal that HGF is active during initiation and progression of pulmonary fibrosis.

Additionally, HGF levels have been described to be increased in the BALF of patients with idiopathic pulmonary fibrosis, sarcoidosis and the interstitial disease associated with rheumatoid arthritis, suggesting a correlation with the diseases outcomes [112]. As shown in the same study using PF model in rats, HGF accelerates lung regeneration [112]. This HGF role was confirmed by a similar study using BLM-induced PF in mice showing that human HGF administration attenuated collagen accumulation [106].

### 1.3.2 HGF/c-Met signaling and immune cells

Besides having well-recognized role as epithelial-specific growth factor and tumor development, role of HGF has also been reported in immune cell functions. Moreover, c-Met expression has been identified in several types of leukocytes, by either presence of c-Met expression and/or cellular responses upon stimulation with HGF indicating that HGF/c-Met signaling can influence leukocyte response during inflammation.

Neutrophil recruitment is an important event in several pathologies, as atherosclerosis, thrombosis, ischemia and pulmonary fibrosis [48]. Recently, it was demonstrated that c-Met expression, induced by inflammatory stimuli, is crucial for neutrophil extravasation to inflamed tumoral tissues modulating and stimulating the firm adhesion of neutrophils to the endothelium [97]. This provides further evidence that c-Met signaling can exert motogenic functions in neutrophils. Moreover, a key role of HGF in the adhesion of neutrophils to endothelial cells has been described, specifically in integrin-mediated adhesion and transmigration of neutrophils to sites of acute inflammation [48]. Once extravasated, HGF/c-Met pathway will still function on neutrophils by reinforcing their cytotoxic response [97]. Recently, it was reported that c-Met inhibition impaired the mobilization and recruitment of neutrophils into tumors and draining lymph nodes in response to cytotoxic immunotherapies. As so, in the absence of c-Met inhibition, neutrophils recruited to T cell-rich areas rapidly acquired immunosuppressive properties, preventing expansion of T lymphocytes and their effector functions [113,114].

Additionally, when isolated monocytes were stimulated with HGF, it was observed an increase in the expression of four chemokines (macrophage inflammatory protein (MIP)-1β, MIP-2α, monocyte chemoattractant protein-1/Ccl2 and IL-8) and other cytokines (IL-4, IL-1β,

macrophage colony-stimulating factor and granulocyte-macrophage colony-stimulating factor) suggesting a proinflammatory role for HGF acting on monocytes [48]. Monocyte activation lead to up-regulation of the c-Met expression in these cells, thus enhancing responsiveness to the factor [115]. This indicates that monocyte function can be modulated by HGF.

Also, c-Met/HGF signals regulate dendritic cells adhesion to the ECM component laminin, however, the antigen-presenting function is not affected [116].

This signaling can also stimulate adhesion and migration of mature memory T cells, however these cells appeared not to express c-Met [117]. More recently it has been describe that while c-Met expression is undetectable in naïve CD8+ T cells, c-Met/HGF pathway control highly cytotoxic CD8+ T cell-mediated anti-tumor immunity [118].

Altogether, the information summarized provides some evidences of the role of c-Met in the modulation of the immune cells and in their mediated effects. Nevertheless, several aspects are still unexplored, namely the c-Met-expressing immune cells in regulation of chronic inflammatory diseases and, in this case, subsequent pulmonary fibrosis.

CHAPTER 2

# RESEARCH OBJECTIVES

# 2. Research Objectives

Lung fibrosis progression has increasingly been associated with immune cells, specifically macrophages and neutrophils. Recently, it has been described that neutrophils recruitment to inflamed tissues is influenced by the expression of a tyrosine kinase receptor, c-Met. In this way, our main goal was to understand how c-Met expression in immune cells influences pulmonary fibrosis progression. To this end, we took advantage of a hematopoietic and endothelial cell-specific c-Met transgenic mouse strain, *c-Met* $^{fl/fl}$/Tie2:Cre-positive, using a BLM-induced lung fibrosis mouse model.

To accomplish the mentioned main goal, the specific objectives of this work were to:

i) Study the effect on lung fibrotic injury, including morphologic and fibrotic lung changes;

ii) Elucidate the influence on inflammatory reaction, including phenotypic identification and quantification of recruited inflammatory cell;

iii) Explore the consequence on critical signaling pathways and inflammatory mediators.

CHAPTER 3

# MATERIALS AND METHODS

# 3. Materials and Methods

## 3.1 Animals

All animal experiments were performed according to the European Union Directive 2010/63/EU and approved by the local ethics committee (SECVS 032/2017). The animals were housed in standard cages (267 x 207 x 140 mm) with 370 $cm^2$ floor area and five animals per cage. The animal room was maintained at 22-24°C, with a relative humidity of 55% and 12h light/dark cycle. Animals were maintained in pathogen-free conditions, under controlled environment, with rodent food diet and water *ad libitum*.

### 3.1.1 Transgenic mice

The transgenic (TG) mice used in this experiment were in C57BL/6J background (supplied by Professor Massimiliano Mazzone, Vesalius Research Center, VIB, KU Leuven, Belgium) and were *c-Met* $^{fl/fl}$/Tie2:Cre positive, which means that Cre recombinase was expressed under the control of Tie2 promoter that excises loxP-flanked *c-Met* gene, resulting in *c-Met* deletion in the hematopoietic and endothelial cells. In wild-type (WT) mice, *c-Met* $^{fl/fl}$/Tie2:Cre negative, Cre recombinase is not expressed and so the deletion did not occur.

The colony was maintained inbreed, WT were crossed with TG mice. Three weeks after birth, an ear tag was put in each animal and 2 mm of tail was collected to perform DNA extraction for genotyping, described in the following section.

### 3.1.2 Genotyping

The piece of tail from three weeks-old mice was incubated with 300 µL of 50 mM sodium hydroxide solution at 98°C for 50 minutes, followed by 15 seconds of vortex and then 30 µL of 1 M tris base solution was added. Samples were centrifuged at 13000 rpm for 6 minutes and DNA containing supernatant was collected to another tube.

The genotyping was performed by polymerase chain reaction (PCR) using Supreme NZYTaq 2x Master Mix (MB05402, NZYTech), specific primers for *Cre* transgene and an endogenous gene as control (Table 3) and 0.5 µL of DNA (≈50 ng/µL).

PCR reaction included the following steps: a first step of 3 minutes at 94°C, 35 cycles of 30 seconds at 94°C, 30 seconds at 62°C and 45 seconds at 72°C and a last step of 5 minutes

at 72°C. PCR products were analysed by electrophoresis in a 2% agarose gel and the following sizes were obtained and used to distinguish the 2 mice groups, TG: 500 base pair (bp) and 420 bp; WT: 420 bp.

**Table 3: Primers used for genotyping PCR.**

| | |
|---|---|
| **Transgene Forward** | 5' CGC-CGT-AAA-TCA-ATC-GAT-GAG-TTG-CTT-C 3' |
| **Transgene Reverse** | 5' GAT-GCC-GGT-GAA-CGT-GCA-AAA-CAG-GCT-C 3' |
| **Positive Control** | 5' CTA-GGC-CAC-AGA-ATT-GAA-AGA-TCT 3' |
| **Positive Control** | 5' GTA-GGT-GGA-AAT-TCT-AGC-ATC-ATC-C 3' |

### 3.1.3 Bleomycin-Induced Pulmonary Fibrosis Mouse Model

WT and TG male mice, between 8- and 10-week-old were used. Analgesics were given by subcutaneous injection of buprenorphine. After 15 minutes anaesthesia was intraperitoneally injected consisting in combination of ketamine and medetomidine. After anaesthesia took effect, a small incision near the throat region of the animals provided access to the tracheal rings and BLM sulphate (BML-AP302-0010, Enzo Life Sciences) intratracheal injection was performed using a 30G needle, as a single dose of 2.5 mg/kg per animal - day 0.

The mice were observed following surgical procedure to ensure they completely recovered from anaesthesia. After surgery, the food was placed on cage' floor, the mice were housed three per cage, 12 hours after surgery analgesic was once more administered. The weight, movements, breathing, fur and healing aspect of the animals were daily monitored. Respiratory failure during surgery and 20% weight loss were established as humane endpoints and once one was reached, mice were sacrificed. Number of animals considered for each set of experimental results and total number of animals subjected to surgery are described in Table 4.

**Table 4: Number of animals used for experimental analysis at the respective time-point after BLM administration.**

| Number of animals | | WT | TG |
|---|---|---|---|
| 3 days | | 12 | 15 |
| 7 days | * | 14 | 14 |
| 14 days | ** | 5 | 6 |
| 21 days | | 24 | 19 |

* Animal subjected to surgery: 23 WT and 17 TG
** Animal subjected to surgery: 11 WT and 16 TG

## 3.2 Survival analysis

After BLM administration animals were followed by a 21-day observation period. Animals' weight was monitored every other day or every 4 days. Mice whose reached one of the humane endpoint, were sacrificed and these data was used to create a survival curve.

## 3.3 Pulmonary Fibrosis Evaluation

At 14 days after BLM administration, mice were anesthetized, perfused with 1x PBS from right to left ventricle of the heart. After dissected, lung lobes were cut in three pieces transverse to the long axis, one of which was fixed for 24 hours in 4% paraformaldehyde (PFA) and proceed to paraffin-embedded samples. The remaining tissue was immediately collected to liquid nitrogen and stored at -80°C.

### 3.3.1 Lung histology and Fibrotic score

Lung sections for histological and fibrotic analysis were cut and stained with hematoxylin and eosin (H&E) and Masson's trichrome, respectively.

The severity of tissue fibrosis was semi-quantitatively assessed based on Ashcroft criteria [119], on the Masson's trichrome stained slides. Briefly, the lung fibrosis was graded on a scale from 0 to 8 by examining whole fields at a magnification of 20x. The grading criteria were as follows: grade 0 - normal lung; grade 1 - minimal fibrous thickening of alveolar or bronchiolar walls; grade 3 - moderate thickening of walls without obvious damage to lung architecture; grade 5 - increased fibrosis with definite damage to lung structure and formation of fibrous bands or small fibrous masses; grade 7 - severe distortion of structure and large fibrous areas; and grade 8 - total fibrous obliteration of fields [119]. Grades 2, 4, and 6 represent intermediates between the afore mentioned criteria. All sections were independently scored by two researchers in a double-blind fashion. The average score from all fields was used to determine the fibrotic score of each animal.

Representative images from the H&E and Masson's trichrome stained tissue sections were acquired using an Olympus BX61 light microscope equipped with an Olympus DP-70 digital camera in a x10 magnification, processed by cellSens software.

### 3.3.2 Hydroxyproline content assay

To estimate the amount of collagen in the lung, lung hydroxyproline content was measured using a hydroxyproline colorimetric assay kit (MAK008, Sigma). Mice lung were weighted and homogenized in 100 µL $H_2O$ per 10 mg tissue in 8 mL capped SVL glass tubes (Pirex), hydrolysed in 6 N HCl at 120°C for 3 hours in a dry block heater (Stuart). Hydrolysed samples were transferred to a 96-well microplate and evaporated to dryness at 70°C. Then, 100 µL of chloramine T reagent was added to each sample and incubated at room temperature (RT) for 5 minutes, followed by the addition of 100 µL of 4-(Dimethylamine) benzaldehyde reagent to each well and incubated at 60°C for 90 minutes. Absorbance of oxidized hydroxyproline was read at 560 nm in a microplate reader Varioskan Flash (Thermo Scientific) and compared to standard curve generated with hydroxyproline standards supplied in the commercial kit. All samples were analysed in duplicate. The amount of collagen was expressed in micrograms per milligram of lung tissue for each animal.

### 3.3.3 Reverse transcriptase-quantitative polymerase chain reaction analysis

#### 3.3.3.1 RNA isolation

RNA from mouse lung tissue was extracted by homogenisation in TRIzol reagent (15596-026, Invitrogen), first through mechanical disruption using microcentrifuge pestle and then needles with crescent gauge values. Homogenate was incubated for 5 minutes at RT, then chloroform was added (0.2 mL per 1 mL of TRIzol used before) and incubated for 3 minutes at RT. Samples were centrifuged at 13000 rpm for 15 minutes at 4°C and aqueous phase was removed, 100% isopropanol was added 1:1 proportion followed by incubation for 10 minutes at RT and centrifuged under the previous settings. Supernatant was discarded, RNA pellet was washed with 70% ethanol and centrifugated at 8000 rpm for 5 minutes at 4°C. Supernatant was discarded, RNA pellet was dried for 15 minutes and then hydrated with RNase-free water.

#### 3.3.3.2 cDNA conversion

To convert 2 µg of RNA it was used the commercial Maxima First Strand cDNA synthesis kit (K1671, Thermo Fisher Scientific), following the manufacturer instructions. Briefly, DNA residues were eliminated using a reaction solution containing 10x DNase Buffer, ds DNase and RNA template at 37°C for 2 minutes. cDNA conversion was performed using a reaction solution containing 5x reaction mix and maxima enzyme, reverse transcriptase, followed by 10 minutes at 25°C, 20 minutes at 50°C and 5 minutes at 85°C.

#### 3.3.3.3 qPCR

1 µL cDNA was mixed with commercial 2x Maxima Probe/ROX Master Mix (K0231, Thermo Fisher Scientific), containing a Hot Start Taq DNA Polymerase and TaqMan® Gene Expression assay, specifically *Gapdh* (Mm99999915_g1), *Col1a1* (Mm00801666_g1), *Col1a2* (Mm00483888_m1), *Col3a1* (Mm00802300_m1), *Acta2* (Mm00725412_s1), *S100a4* (Mm00803372_g1), *Tgf-β1* (Mm01178820_m1), *Ctgf* (Mm01192933_g1), *Eln* (Mm0051470_m1) and *Igf-1* (Mm00439560_m1). Quantitative PCR (qPCR) thermocycler program was 10 minutes at 95°C, 40 cycles of 15 seconds at 95°C and 30 seconds at 60°C.

Transcript' levels were normalized to endogenous control *Gapdh* and transcript' expression levels analysis was performed accordingly to $2^{-\Delta\Delta CT}$ method [120]. Gene expression data was presented in relative transcript' expression fold-change based on: $2^{-\Delta\Delta CT}$ (individual value) / average ($2^{-\Delta\Delta CT}$ (WT group)). Each experiment was conducted in duplicate and the expression results are presented in fold-change. Statistical analysis was performed using relative transcript' expression fold-change from WT group versus relative transcript' expression fold-change from TG group.

## 3.4 Inflammatory response evaluation

At 3 and 7 days after BLM administration, mice were anesthetized and perfused with 1x PBS from right to left ventricle of the heart. By day 7 bronchoalveolar lavage fluid was collected as detailed below and the tissue was dissociated for flow cytometry analysis and remaining cells were stored at -80°C. By day 3 the tissue was dissociated for flow cytometry analysis.

### 3.4.1 Bronchoalveolar lavage

BALF was recovered from each mouse. Briefly, the trachea was cannulated with 25G needle (450090, Greiner Bio-One Vacuette), the lungs instilled with of 1 mL of 1x PBS and 80% to 90% of the fluid withdrawal. This procedure was repeated twice. Then BALF were centrifuged at 1500 rpm for 5 minutes 4°C, supernatant was collected and stored at -80°C for the analysis described in 3.4.3. The pellet was resuspended in Ammonium-Chloride-Potassium (ACK) lysis buffer (A1049201, Gibco), which was then incubated at RT for 4 minutes, by the end of this incubation 1x PBS was added before being re-centrifuged under the previously determined settings. The supernatant was discarded, and the pellet resuspended in PBS with 4% FBS (FACS buffer). Approximately 1,000,000 cells from each specimen were loaded onto a cytometer tube and proceeded to flow cytometry staining described in 3.4.4.

### 3.4.2 Lung dissociation

After dissection, the lungs were placed in dispase while minced into 2-3 $mm^3$ pieces for 10 minutes at RT. Then DNase (10104159001, Roche) and collagenase (17101-015, Gibco) solution (DNase I 1 mg/mL and Collagenase II 5 mg/mL in Dulbecco's Modified Eagle Medium - DMEM) was added to the sample. After, an enzymatic digestion period of 10 minutes at 37°C, tissue disruption was performed by several mechanical titrations with P1000 tip, and then the sample was returned for a second incubation period of 10 minutes at 37°C. After incubation, the disrupted tissue suspension was collected and discarded through a 100 µm cell strainer suspended over a 50 mL tube. The petri dish was washed with DMEM/20% FBS to ensure maximum retrieval of cells and the fluid was discharged through the cell strainer. The remaining tissue in the strainer was dissociated mechanically using the black back of a syringe before washing the strainer with DMEM/20% FBS. Then the suspension was passed through a 70 µm strainer, washed again and centrifuged at 1500 rpm for 5 minutes at 4°C. The supernatant was collected and stored at -80°C for the analysis described in 3.4.3 and the pellet was resuspended in ACK lysis buffer (A1049201, Gibco), which was then incubated at RT for 4 minutes, by the end of this incubation 1x PBS was added before being re-centrifuged under the previously determined settings. The supernatant was discarded, and the pellet resuspended in FACS buffer for the analysis described in 3.4.4.

### 3.4.3 Lactate Dehydrogenase assay

The lactate dehydrogenase (LDH) activity in the BALF and tissue homogenate supernatants was evaluated as a marker of cytotoxicity, assayed using the LDH kit (K726, BioVision) and read out by a standard spectrophotometric method. Briefly, 2 µL supernatant were transferred to a 96-well plate and 100 µL of LDH substrate mixture were added, the absorbance was measured at the wavelength of 450 nm in a microplate reader Varioskan Flash (Thermo Scientific) and compared to standard curve generated with NADH standards supplied in the commercial kit. Then the plate was incubated for 30 minutes at 37°C. All samples were analysed in duplicate. The LDH activity was expressed in nmol/min (mU) per mL.

### 3.4.4 Flow Cytometry staining

An aliquot of each single-cell suspensions from each animal group containing $1x10^6$ cells was loaded into a cytometer tube, which was centrifuged at 1500 rpm for 5 minutes at 4°C. The

supernatant was removed and the pellet resuspended in FACS buffer containing fluorochrome-conjugated antibodies, as indicated in Table 5, and incubated for 30 minutes in the dark. The cell suspension was then washed with FACS buffer, centrifuged and supernatant discarded as above. The cell pellets were resuspended in 100 µL of PBS containing 0.1 µL of Viable Dye eFluor® 450 (65-0863-14, Ebioscience) and incubated for 30 minutes. The cell suspension was washed and centrifuged as above mentioned. The supernatant was discarded and after fixation in 200 µL of 4% PFA for 30 minutes, the pellet was resuspended in 250 µL FACS buffer solution by tapping. Finally, the cells were analysed in the LSR II flow cytometer system (BD Bioscience).

**Table 5: Primary antibodies and respective concentration used for flow cytometry analysis.**

| Antibody<br>Host specie – Reactivity | Fluorochrome<br>Reference | Concentration |
|---|---|---|
| CD45<br>rat anti-mouse | PE-Cy7<br>552848, BD | 1/200 |
| F4/80<br>rat anti-mouse | PerCP/Cy5.5<br>45-4801-80, Ebioscience | 1/200 |
| CD11c<br>hamster anti-mouse | PE<br>117307, Biolegend | 1/100 |
| Ly-6G<br>rat anti-mouse | BV 605<br>127639, Biolegend | 1/100 |
| CD11b<br>human anti-mouse | BV 711<br>101241, Biolegend | 1/100 |
| CD3<br>rat anti-mouse | APC<br>100236, Biolegend | 1/100 |
| CD19<br>rat anti-mouse | APC/Cy7<br>115530, Biolegend | 1/100 |
| Ly-6C<br>rat anti-mouse | BV 500<br>128033, Biolegend | 1/100 |

Autofluorescence background was checked and voltages were set with the unstained control and compensations were performed using AbC Total Antibody Compensation Kit (A10497, life technologies) for each fluorochrome. 50.000 CD45+ events were obtained per sample and analysed using FlowJo Software (Tree Star, Ashland, OR, USA) as outlined in Figure 8. Dead cells were identified by positive viability dye staining and excluded from the analysis. We defined cell compartments by populations outlined in Figure 8 and in Table 6:

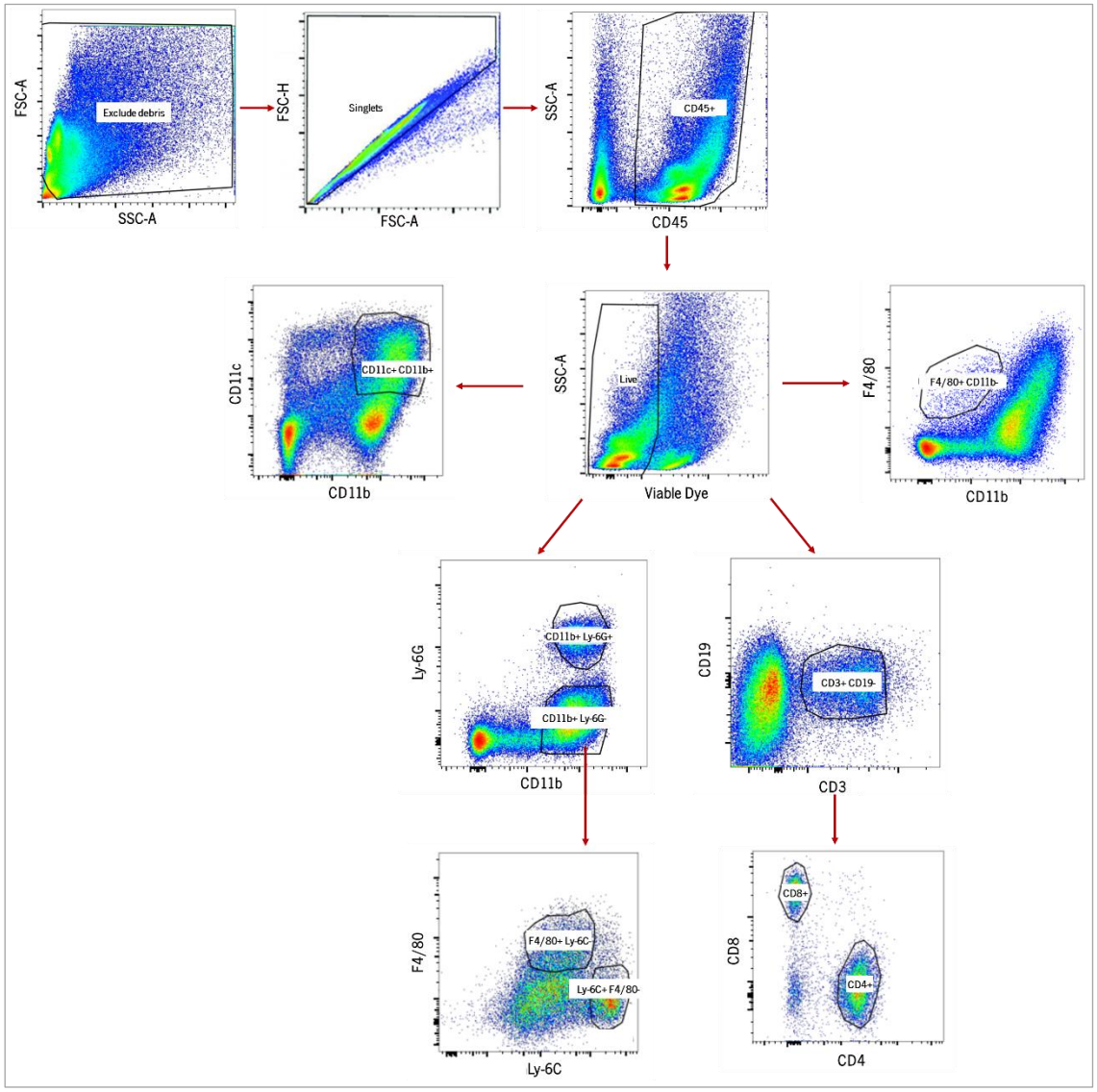


**Figure 8: Gating strategy to identify myeloid- and lymphoid-cell subsets in mice lung at day 7 after mice treatment with BLM.**

Gating for exclusion of debris and doublets were performed using forward vs side scatter area (FSC-A vs SSC-A) and FSC-A vs FSC height area plot, respectively. Then $CD45^+$ population (leukocytes) was gated and subsequently the viable status to exclude dead cells. CD11b and CD11c status were assessed to identify alveolar macrophages/ dendritic cells ($CD11b^+CD11c^+$). Ly-6G and CD11b status were assessed to identify neutrophils ($CD11b^+Ly\text{-}6G^+$) and Ly-6G negative population was assessed to identify monocytic-derived tissue macrophages ($CD11b^+Ly\text{-}6G^-F4/80^+Ly\text{-}6C^-$) and monocytes ($CD11b^+Ly\text{-}6G^-F4/80^-Ly\text{-}6C^+$). F4/80 and CD11b status were assessed to identify resident macrophages ($CD11b^-F4/80^+$). CD19 and CD3 status were assessed to identify T cells ($CD3^+CD19^-$), CD4 T cells ($CD3^+CD4^+CD8^-CD19^-$) and CD8 T cells ($CD3^+$ $CD8^+CD4^-CD19^-$).

Table 6: Populations established for myeloid and lymphoid cells identification.

| Cell type | Markers |
|---|---|
| Alveolar Macrophages/ Dendritic Cells | $CD11b^+$ $CD11c^+$ |
| Neutrophils | $CD11b^+$ $Ly\text{-}6G^+$ |
| Monocytic-derived Resident Macrophages | $CD11b^+$ $Ly\text{-}6G^-$ $F4/80^+$ $Ly\text{-}6C^-$ |
| Monocytes | $CD11b^+$ $Ly\text{-}6G^-$ $F4/80^-$ $Ly\text{-}6C^+$ |
| Resident Macrophages | $CD11b^-$ $F4/80^+$ |
| T cells | $CD3^+$ $CD19^-$ |
| CD4 T cells | - $CD3^+$ $CD4^+$ $CD8^-CD19^-$ |
| CD8 T cells | - $CD3^+$ $CD8^+$ $CD4^-CD19^-$ |

## 3.4.5 Reverse transcriptase-quantitative polymerase chain reaction analysis

### 3.4.5.1 RNA isolation

Total RNA from murine lung cells was isolated using ExtractMe total RNA Kit (EM09, Blirt) according to the manufacturer instructions. Briefly, in the first step, the tissue was homogenized in 600 µL of lysis buffer, then the homogenate was lysed mechanically and undigested cells that remain were discarded after centrifugation at 13000 rpm for 2 minutes. After equal volume ethanol addition RNA attached to a purification column membrane. On-column, treatment with DNase I removed the remaining genomic DNA. Finally, impurities and enzyme inhibitors were removed in a three-step washing stage and then purified RNA was eluted with the appropriated buffer.

### 3.4.5.2 cDNA conversion

Performed as described in section 3.3.3.2.

### 3.4.5.3 qPCR

Performed as described in section 3.3.3.3, using TaqMan® Gene Expression assay, specifically *Gapdh* (Mm99999915_g1), *IL-1β* (Mm00434228_m1), *IL-6* (Mm01168134_m1), *IL-10* (Mm01288386_m1), *Ifn-γ* (Mm01168134_m1), *Igf-1* (Mm00439560), *Tnf-α* (Mm00443258_m1), *Tgfβ1* (Mm01178820_m1), *Ccl2* (Mm00441242_m1), *IL-4*

(Mm00445259_m1), *Ccl3* (Mm00441259_g1), *Ctgf* (Mm01192933_g1) and *iNOS* (Mm00440502_m1).

## 3.5 Statistical Analysis

All statistical analyses were performed using GraphPad Prism, version 5.0 (GraphPad Software, San Diego, CA). Data were presented as mean±standard error of the mean (SEM). Differences between two groups were analysed using Student's t-test. Kaplan-Meyer survival analysis was compared by log-rank test. The level of significance in all statistical analysis was set at *p<0.05.

## 3.6 Experimental design

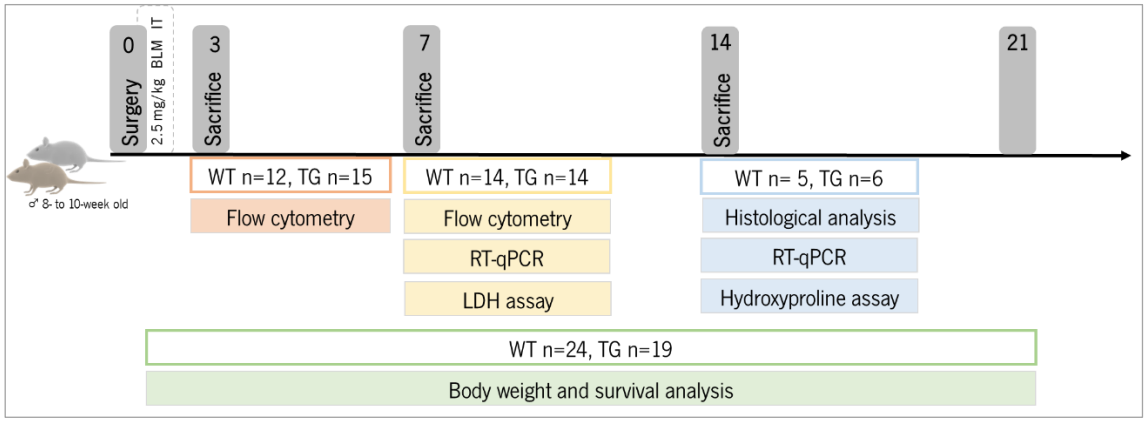


**Figure 9: Experimental design.**

Timeline of the experimental procedures performed, respective time-points and analysis performed in each. At day 0 intratracheal (IT) administration was performed, followed by the sacrifice at specific time-points, tissue collection and respective analysis.

CHAPTER 4

# RESULTS

# 4. Results

Lung fibrosis progression has increasingly been associated with chronic inflammation, particularly neutrophils and macrophages. Recently, c-Met expression in neutrophils upon inflammatory stimulation has been described as essential for their extravasation to inflamed tumors. However, contribution of c-Met expression in immune cells to pulmonary fibrosis progression is unknown. In this thesis the main purpose was to understand the influence of c-Met expression in immune cells during inflammation-associated and fibrogenic process in BLM-induced pulmonary fibrosis. For that *c-Met*-deletion in immune and endothelial cells was used, by a genetic approach specifically targeting the Tie2 lineage, to clarify the main alterations regulated by c-Met-expressing immune cells across lung fibrosis progression.

## 4.1 Influence of c-Met-expressing immune cells on long-term effects of lung fibrosis

BLM-induced lung injury model in mice is characterized by extensive fibrosis 14–28 days after a single administration, causing impaired respiratory function and ultimately significant morbidity and mortality [88]. To understand the influence of c-Met-expressing immune cells on the long-term effects, namely physical health and survival of mice during the progression of BLM-induced lung fibrosis, we followed the survival and weight loss for 21 days after BLM intratracheal administration.

The survival in the WT group was 20.8±8.29% (5/24), while the TG group showed significantly higher rates 57.9±11.3% (11/19) (p=0.009) by day 21 (Figure 10). On day 3, 1 WT animal was sacrificed, as so decreasing the survival to 95.8±4.08%. The highest mortality occurred by day 5, 13 WT and 4 TG mice were sacrificed, as so survival decreased to 41.7±10.1% in WT group and to 78.9±9.35% in TG group (WT- 10/24; TG- 15/19). By day 8, 2 WT mice were sacrificed, diminishing the survival to 33.3±9.62%. Regarding TG animals, 3 were sacrificed by day 9, decreasing the survival to 63.2±11.1% and by day 12, 1 animal was sacrificed decreasing survival to the final rate of 57.9±11.3%. 1 WT mice animal was sacrificed at day 11, decreasing the survival to 29.2±9.28% and 2 by day 18, reducing the survival to the final rate of 20.8±8.29%.

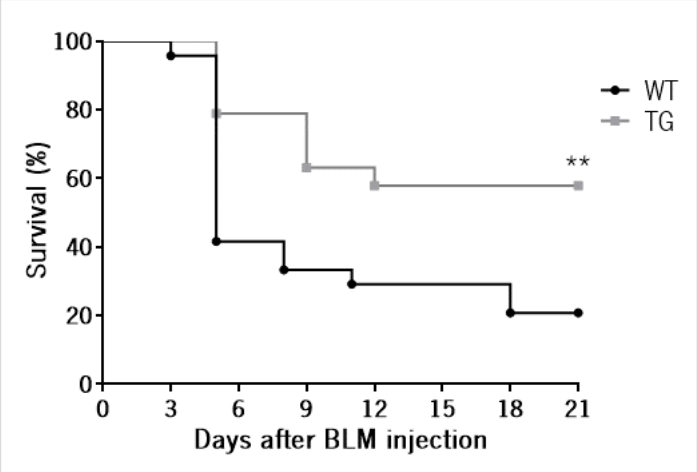


**Figure 10: Kaplan-Meier survival curves of mice until day 21 after BLM intratracheal injection.**
BLM was administered on day 0 followed by a 21-day observation period (**p<0.01 by the log-rank test).

Average body weight at day 0 did not differ between both groups (WT- 30.6±2.1 g; TG- 30.0±3.7 g, p=0.62) (Figure 11). During the first week after BLM administration both WT and TG mice lost weight, reaching their lowest point on the eighth day after surgery (WT- 21.9±1.9 g, TG- 22.5±5.4 g, p=0.82). After this week, TG mice gradually recovered body weight, while WT presented a slight decrease until day 21. The statistical differences between both groups' body weight were observed from day 11 (WT- 21.1±1.8 g, TG- 24.5±3.2 g, p=0.047) onwards. By day 21 the average body weight in WT group (19.5±0.1 g) was significantly lower than in TG group (30.2±1.7 g, p=0.014), representing a difference of 58% in body weight.

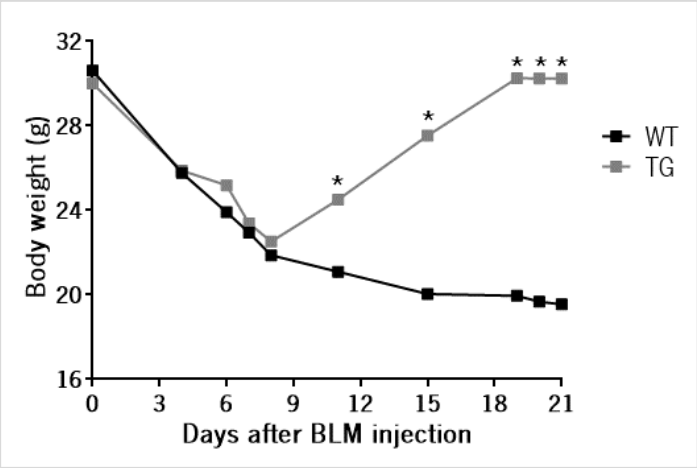


**Figure 11: Mice body weight during 21 days after BLM administration.**
Time-course of body weight changes in WT and TG mice after administration of BLM (*p < 0.05).

These results suggest that *c-Met* deletion in immune cells was protective against the long-term effects induced by pulmonary fibrosis.

## 4.2 Impact of c-Met-expressing immune cells in fibrogenic processes

### 4.2.1 Lung morphology and collagen content

BLM-induced lung injury model in mice is characterized by extensive fibrosis, causing impaired gas exchange due to destruction of alveolar structures, through excessive ECM and collagen deposition within lung interstitium [88].

As so next, we intended to clarify the influence of c-Met-expressing immune cells in the extent of tissue destruction and fibrotic lesion at day 14 after BLM administration. For that, we performed histological analysis of H&E stained-lung sections (Figure 12A) as well as fibrotic lesion extension (Figure 12B) and respective quantification through Masson's Trichrome stained-lung sections based on a fibrotic score criteria (Figure 12C).

Histologically, WT mice presented more fibrotic areas composed by hyperproliferative cells, with more extensive destruction of alveolar architecture and loss of alveolar surface area, also with larger agglomerates of inflammatory cells (Figure 12A). While TG mice presented smaller areas of hyperproliferation and preserved alveolar structure. Moreover, considering the fibrotic lesion TG mice presented less abundant collagen deposition (Figure 12B, arrow head) and more preserved alveolar walls thickness with less parenchymal destruction (Figure 12B, arrow) compared to WT mice. Ashcroft score [119] (Figure 12C) was consistent with morphological analysis, showing significant difference between WT and TG mice, with TG mice presenting 51% lower score (3.97±0.24 vs 1.95±0.37, p=0.002).

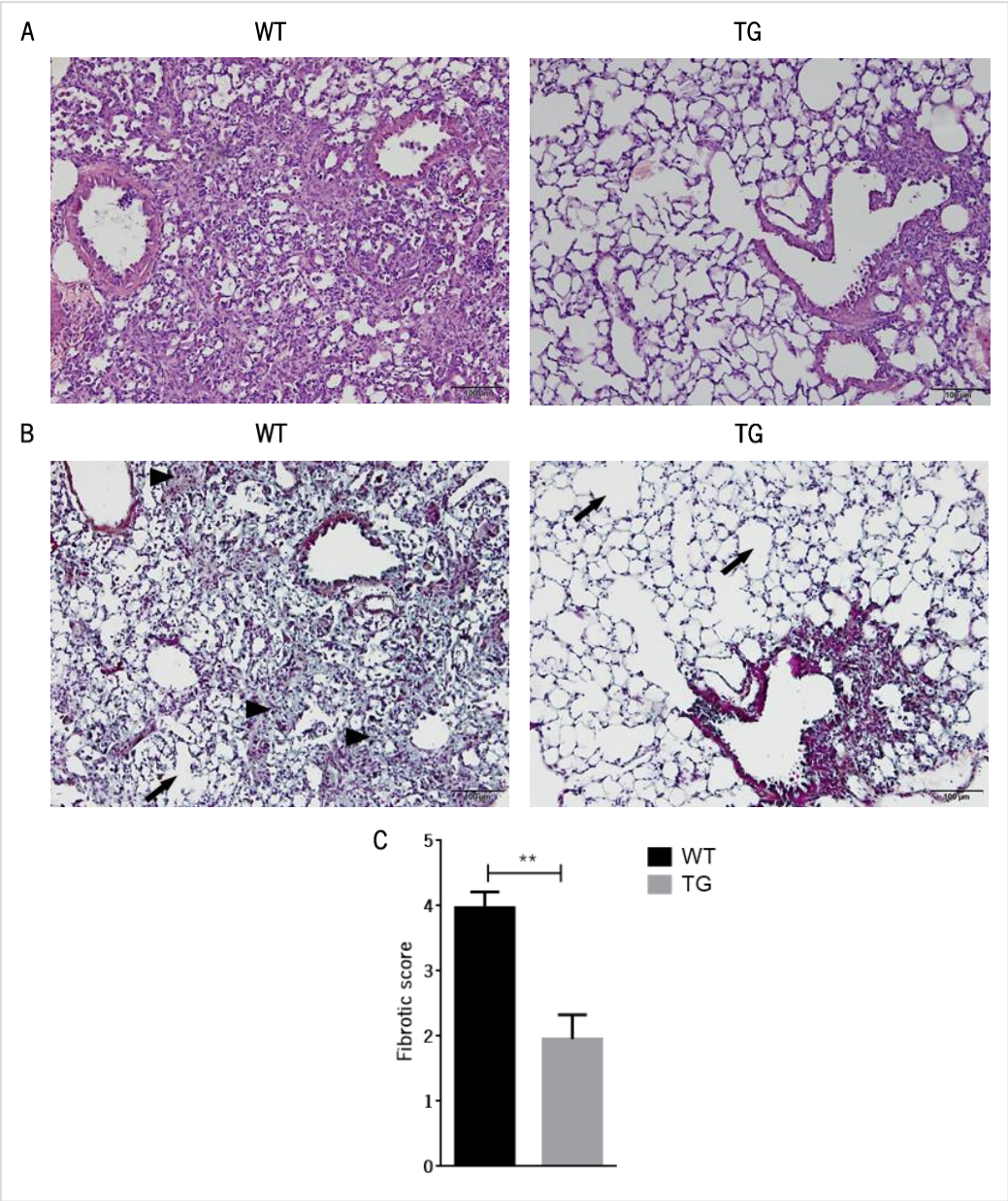


**Figure 12: Histological analysis of BLM-induced lung injury at day 14 after intratracheal BLM administration.**

Representative images from (A) H&E and (B) Masson's trichrome staining of WT and TG mice lung sections. (C) Semi-quantification of lung fibrosis using Ashcroft's criteria was performed in WT and TG mice. The photos were taken at x10, scale bars of images: 100 µm (arrow indicates parenchymal destruction, arrow head indicates collagen deposition, **p<0.01).

Hydroxyproline is an aminoacid exclusively found in collagen which content partly reflects the degree of lung fibrosis. Thus, to more precisely quantify the collagen deposition levels we measured total hydroxyproline levels in lung homogenates from WT and TG mice (Figure 13). Although not statically significant, we detected a considerable decrease trend in hydroxyproline content in TG mice compared to WT mice, representing a 42% decrease (0.69±0.11 µg/g of tissue vs 0.40±0.064 µg/g of tissue, p=0.053).

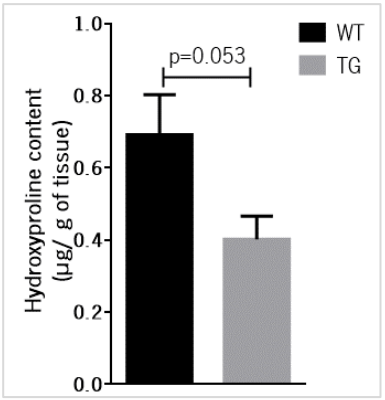


**Figure 13: Collagen content analysis of mice lung at day 14 after BLM administration.**
Quantification of total hydroxyproline content of lungs was performed in WT and TG mice.

Overall, these result show that c-Met expression in immune cells influences the fibrotic extent severity and associated collagen deposition in lung fibrosis.

### 4.2.2 Transcript' expression analysis of ECM components, stromal cells and profibrotic mediators

Fibrosis is a basic connective tissue lesion defined by the increase in the amount of tissue fibrillar ECM components [20]. In this way to confirm the decrease in collagen deposition observed in TG mice, we assessed the transcript' levels of collagens, namely *collagen I $\alpha$ 1* (*Col1a1*), *collagen I $\alpha$ 2* (*Col1a2*) and *collagen III $\alpha$ 1* (*Col3a1*) and other ECM components, as *elastin* (*Eln*). This analysis was performed in whole lung tissue on day 14 post-BLM administration in WT and TG mice (Figure 14).

Although *Eln* (0.93±0.12, p=0.58) and *Col3a1* (0.87±0.051, p=0.092) expression levels were not altered in TG mice compared to WT mice (*Eln*- 1.02±0.098; *Col3a1*- 1.00±0.044), the expression levels of both *Col1a1* and *Col1a2* were significantly decreased in TG mice (0.68±0.047, p=0.0002 and 0.77±0.028, p=0.002, respectively) having as control the expression levels obtained in WT mice (*Col1a1*- 1.00±0.017; *Col1a2*- 1.00±0.044). This result is consistent with the histological finding of decreased collagen deposition in TG mice.

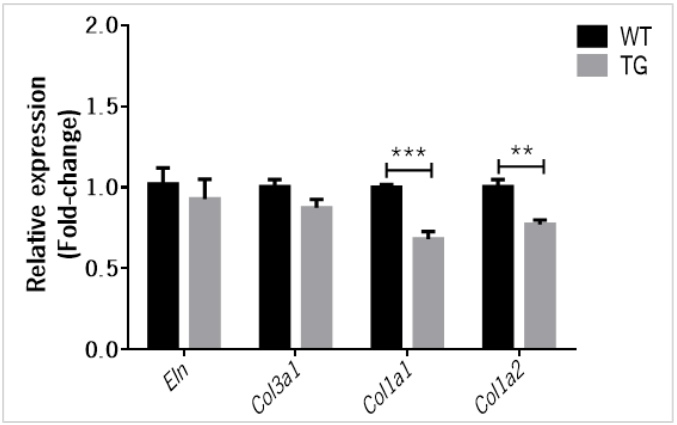


**Figure 14: Transcript' expression analysis of ECM components at day 14 after mice treatment with BLM.**
ECM components (*Eln, Col3a1, Col1a1, Col1a2*) transcript' levels were analysed in WT and TG mice lungs by qPCR. Expression levels were normalized to *Gapdh*. Data presented as mean±SEM (**p<0.01, ***p<0.001).

The fibroblasts and myofibroblast are major producers of ECM, being responsible for its accumulation [49]. To evidence the presence of these cells, the levels of relative transcript' expression of suitable markers of these interstitial matrix-producing cells were determined in whole lung tissue at day 14 post-BLM administration (Figure 15). *S100a4*, a fibroblastic marker, transcript' levels were statistically reduced in TG mice, representing a 31% reduction (0.69±0.067 vs 1.00±0.074, p=0.021). On the other hand, no differences were observed on expression levels of activated myofibroblasts, smooth muscle actin (*Acta2*), in TG mice (1.34±0.10 vs 1.04±0.14, p=0.11) having as control the expression levels obtained in WT mice.

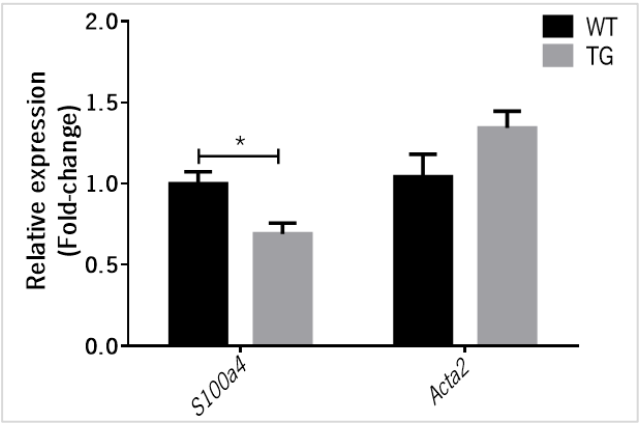


**Figure 15: Transcript' expression analysis of stromal cell markers at day 14 after mice treatment with BLM.**
Fibroblasts (*S100a4*) and myofibroblasts (*Acta2*) transcript' levels were analysed in WT and TG mice lungs by qPCR. Expression levels were normalized to *Gapdh*. Data presented as mean±SEM (*p < 0.05).

Furthermore, there are some growth factors that have been implicated in the development and progression of pulmonary fibrosis, namely Tgf-β1, Igf-1 and Ctgf, known for their ability to

stimulate fibroblast activation, differentiation and ECM production [28]. In this way, we intended to elucidate whether these factors were altered in *c-Met*-deleted immune cells mice (Figure 16).

Interestingly, regarding transcript' expression of profibrotic genes, only *Igf-1* expression was found to be significantly diminished, 42%, in the immune cells *c-Met*-lacking mice (0.58±0.052 vs 1.00±0.061, p=0.0007), while *Tgf-β1* and *Ctgf* expression levels were not altered in TG mice (1.14±0.076 vs 1.00±0.063, p=0.22 and 0.90±0.079 vs 1.00±0.038, p=0.30, respectively), having as control the expression levels obtained in WT mice.

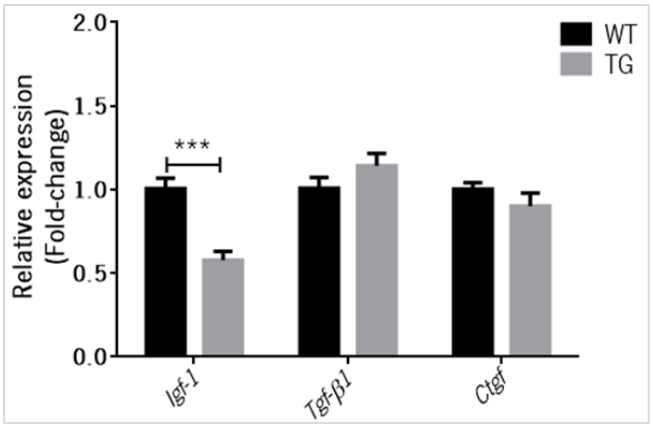


**Figure 16: Transcript' expression analysis of profibrotic factors at day 14 after mice treatment with BLM.**
Profibrotic factors (*Igf-1, Tgf-β1, Ctgf*) transcript' levels were analysed in WT and TG mice lungs by qPCR. Expression levels were normalized to *Gapdh*. Data presented as mean±SEM (***p<0.001).

Overall, these data indicate that c-Met expression in immune cells impacts fibrogenic processes.

## 4.3 Effect of c-Met-expressing immune cells in inflammation-associated fibrosis

### 4.3.1 Tissue cytotoxicity and inflammatory cells recruitment

Lung damage associated with fibrosis, as in BLM-induced lung injury, is commonly initiated by DNA damage that could result on cellular necrosis and release of intracellular contents into the extracellular space which lead to an exacerbated inflammatory response resulting in tissue cytotoxicity [90]. The inflammatory process is closely related with this initial tissue cytotoxicity and lately the disease severity. Therefore, we decided to investigate the effects of *c-Met*-deletion in immune cells in the cytotoxic environment, as a readout of tissue damage, during the first phase

of BLM-induced lung fibrosis at day 7 after BLM administration. For these purpose, LDH activity was used to evaluate the cytotoxicity in BALF and tissue homogenate supernatant (Figure 17A and B, respectively).

TG mice presented around 40% lower LDH levels, being this decrease statistically significant both in BALF (5.37±1.04 mU/mL) and tissue homogenate supernatant (111±14.9 mU/mL), compared to WT mice (9.50±1.17 mU/mL, p=0.019; 174±11.7 mU/mL, p=0.005).

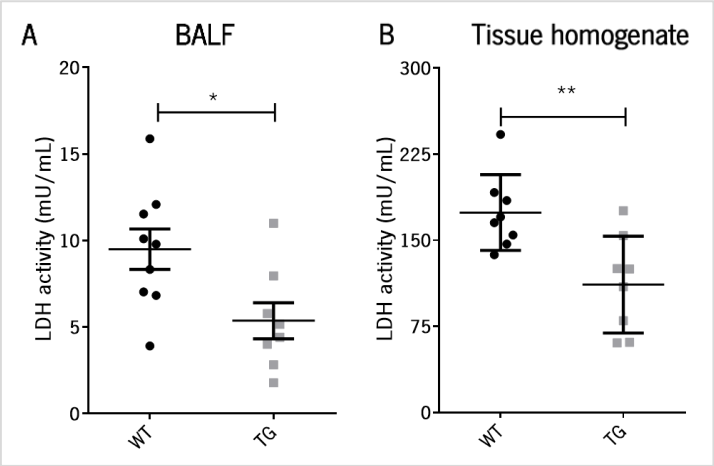


**Figure 17: Tissue cytotoxic analysis at day 7 after mice treatment with BLM.**

LDH activity measured with a colorimetric assay as a cytotoxic marker in (A) BALF and (B) tissue homogenate supernatant for each group. Data are expressed as mean±SEM (*p < 0.05, **p<0.01).

As previously demonstrated by several studies, IPF pathogenesis is characterized by the infiltration of inflammatory cells to the lungs, thus playing an essential role in disease severity [50]. Myeloid cells besides contributing to the severity of the pulmonary fibrosis, are at the same time involved in the tissue repair [121]. These together with the previous results, which show that TG mice showed attenuated later events and decreased initial tissue cytotoxicity, raise the next addressed question, whether inflammatory recruitment after lung injury was affected in the late (7 days) and early (3 days) inflammatory phase of disease progression. Thus, we analysed the inflammatory cells at day 7 after BLM treatment in the BALF (Figure 18) and at day 7 and 3 in the whole lung tissue by flow cytometry (Figure 19).

Regarding cellular characterization of BALF cells at day 7 after BLM treatment we found that neutrophils present a tendency of 40% toward lower number in TG mice compared to WT (1383±266 vs 2357±559, respectively, p=0.18) (Figure 18A), but without statistically significant

difference. Moreover, any differences were found in the remaining cell types studied, namely monocytic-derived resident macrophages (387±55.9 vs 433±86.2, p=0.66) (Figure 18B), alveolar macrophages/dendritic cells (571±101 vs 547±80.6, p=0.86) (Figure 18C), monocytes (214±39.9 vs 163±34.5, p=0.36) (Figure 18D), resident macrophages (181±50.6 vs 122±50.6, p=0.42) (Figure 18E), T cells (739±138 vs 617±105, p=0.51) (Figure 18F), CD4 T cells (476±82.6 vs 417±83.7, p=0.62) (Figure 18G) and CD8 T cells (97.7±30.0 vs 79.8±16.6, p=0.62) (Figure 18H).

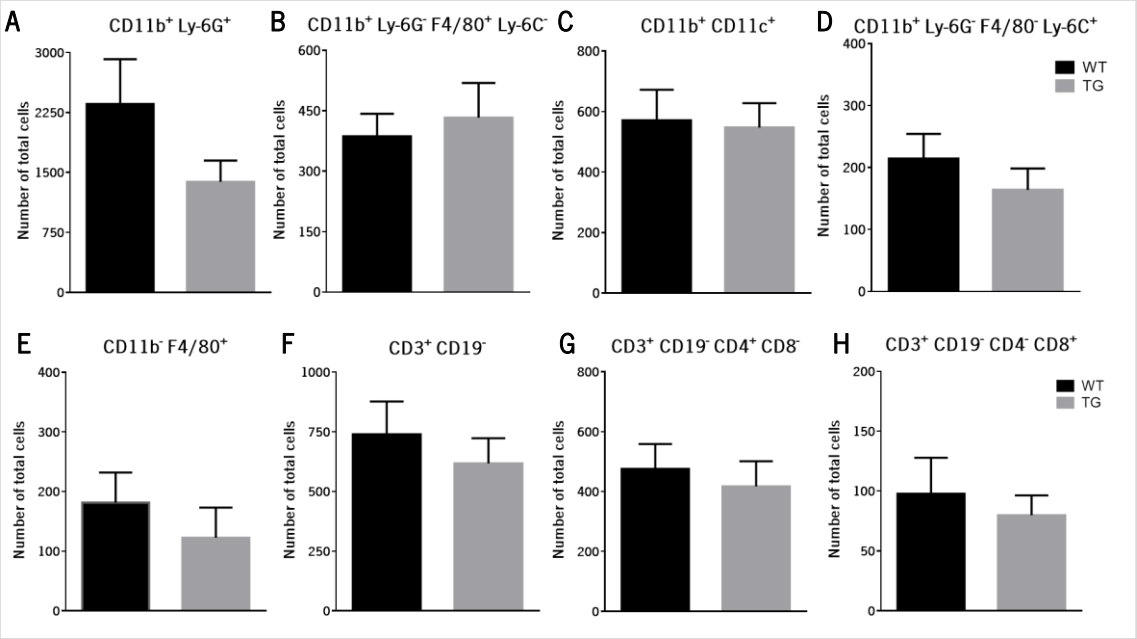


**Figure 18: Inflammatory cells profile from BALF at day 7 after mice treatment with BLM.**

The immune cell populations analysed were (A) CD11b+Ly-6G+, neutrophils, (B) CD11b+Ly-6G-F4/80+Ly-6C-, monocytic-derived resident macrophages, (C) CD11b+CD11c+, alveolar macrophages/dendritic cells, (D) CD11b+Ly-6G-F4/80-Ly-6C+, monocytes, (E) CD11b-F4/80+, resident macrophages, (F) CD3+CD19-, T cells, specifically (G) CD3+CD19-CD4+CD8-, helper T cell, and (H) CD3+CD19-CD4-CD8+, cytotoxic T cell, in WT and TG mice lungs by flow cytometry. Data presented as mean±SEM.

Regarding the inflammatory infiltrate in the lung interstitium, at day 7 after BLM administration, we found neutrophil number is reduced in TG mice compared to WT (14822±3271 vs 28322±6071, respectively, p=0.049) (Figure 19A). Furthermore, similarly, monocytic-derived resident macrophages in the whole lung tissue of TG mice were significantly diminished compared to WT (1640±398 vs 3616±639, respectively, p=0.014) (Figure 19B). No other significant difference were observed between genotypes 7 days after BLM-treatment in whole lung, namely alveolar macrophages/dendritic cells (11095±2075 vs 11097±2426, p=0.99) (Figure 19C), monocytes (5186±749 vs 4432±962, p=0.54) (Figure 19D), resident macrophages (781±228 vs 555±137, p=0.38) (Figure 19E), T cells (15851±1445 vs 14196±1405, p=0.42) (Figure 19F),

CD4 T cells (7952±2094 vs 8824±1190, p=0.71) (Figure 19G) and CD8 T cells (2792±627 vs 3144±388, p=0.62) (Figure 19H).

These results indicate that *c-Met* deletion in immune cells influences the number of monocytic-derived resident macrophages and neutrophils at the late inflammatory phase of BLM-induced lung fibrosis, from which presence can be associated with a worsened disease outcome verified in WT mice.

To evaluate an earlier inflammatory time-point and compare the cellular recruitment with the disease progression, a set of animals was sacrificed on day 3 after BLM administration. Although at day 3 no differences were found between genotypes in any cell type assessed, changes in the cell number during disease time-course were detected. Interestingly, number of neutrophils significantly increase in WT mice from day 3 to 7 (12405±1832 vs 28322±6071, p=0.013) while in TG no differences were found compared to day 7 (14839±1286 vs 14822±3271, p=0.99) (Figure 19A). The same pattern was observed in T cells comparing day 3 with day 7 post-BLM administration (WT- 10617±810 vs 15851±1445, p=0.005; TG- 12042±1420 vs 14196±1405, p=0.30) (Figure 19F). Regarding alveolar macrophages/ dendritic cells a considerable increase from day 3 to 7 was found in both genotypes (WT- 665±104 vs 11095±2075, p<0.0001; TG- 594±72.5 vs 11097±2426, p<0.0001) (Figure 19C), similarly to monocytic-derived resident macrophages, despite being this increase more significant in WT mice (WT- 262±20 vs 3616±639, p<0.0001; TG- 258±21 vs 1640±398, p=0.001) (Figure 19B). No differences in the remaining cell types were found between the same genotype comparing day 3 and 7 days after BLM-treatment, namely monocytes (WT- 3991±484 vs 5186±749, p=0.21; TG- 4970±431 vs 4432±962, p=0.61) (Figure 19D), resident macrophages (WT- 890±81.8 vs 781±228, p=0.66; TG- 901±104 vs 555±137, p=0.05) (Figure 19E), CD4 T cells (WT- 6973±520 vs 7952±2094, p=0.55; TG- 7781±1001 vs 8824±1190, p=0.53) (Figure 19G) and CD8 T cells (WT- 2715±262 vs 2792±627, p=0.89; TG- 3197±394 vs 3144±338, p=0.93) (Figure 19H). These results showed that the influx of neutrophils and T cells is higher in WT mice and that the recruitment of alveolar macrophages/dendritic cells as well as inflammatory macrophages is increased in both genotypes. Taken together, these data point towards an attenuated recruitment of inflammatory cells in TG mice upon treatment with BLM, suggesting that c-Met expression in neutrophils and monocytic-derived macrophages is regulating their infiltration during inflammatory phase of pulmonary fibrosis.

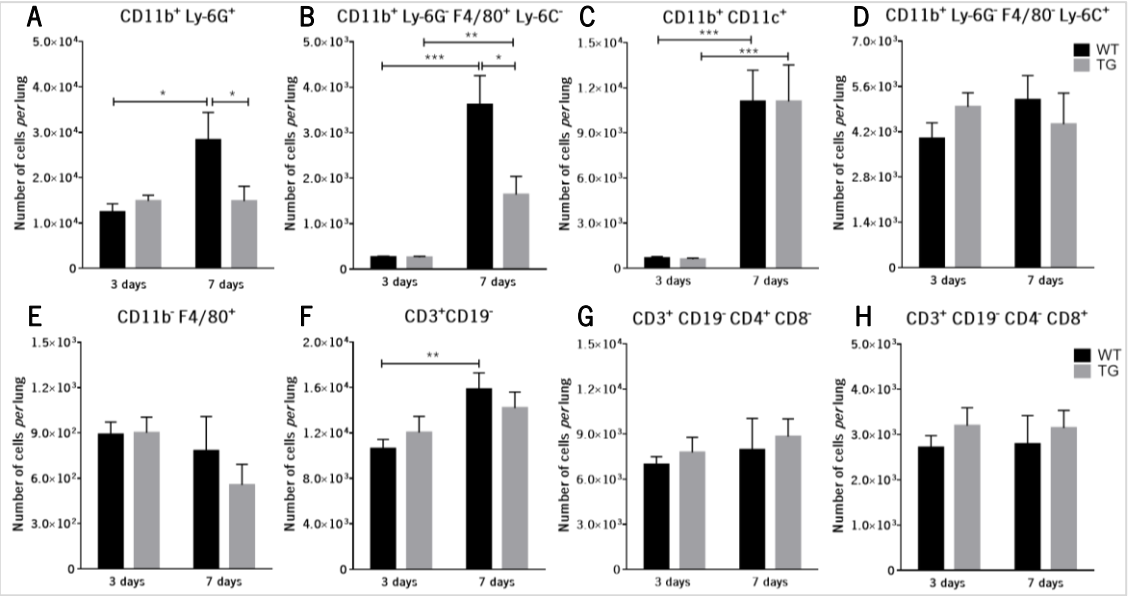


**Figure 19: Characterization of pulmonary infiltration by inflammatory cells at day 3 and 7 after mice treatment with BLM.**

The immune cell populations analysed were (A) CD11b+Ly-6G+, neutrophils, (B) CD11b+Ly-6G-F4/80+Ly-6C-, monocytic-derived resident macrophages, (C) CD11b+CD11c+, alveolar macrophages/dendritic cells, (D) CD11b+Ly-6G-F4/80-Ly-6C+, monocytes, (E) CD11b-F4/80+, resident macrophages, (F) CD3+CD19-, T cells, specifically (G) CD3+CD19-CD4+CD8-, helper T cell, and (H) CD3+CD19-CD4-CD8+, cytotoxic T cell, in WT and TG mice lungs by flow cytometry. Data presented as mean±SEM (*$p < 0.05$, **$p<0.01$, ***$p<0.001$).

### 4.3.2 Transcript' expression analysis of inflammatory and fibrotic mediators

In the disease progression, a complex network of inflammatory cytokines and cell types favors the recruitment of immune cells and fibroblasts. Subsequently, we assessed the transcript' levels of some important cytokines and growth factors mediating the fibrosis progression.

For this at day 7 post-BLM administration expression levels of cytokines, namely anti-inflammatory (*IL-10 and IL-4*) and proinflammatory (*Ifn-γ, Ccl2, Ccl3, Tnf-α, IL-6, IL-1β, iNos*) were determined in whole lung tissue (Figure 20). We found that gene expression levels of the anti-inflammatory cytokines, *IL-10* (1.51±0.29 vs 1.00±0.18, p=0.14) and *IL-4* (2.22±0.6 vs 1.00±0.22, p=0.063), also some proinflammatory cytokines, specially *Ifn-γ* (1.84±0.55 vs 1.00±0.19, p=0.11), *Ccl2* (1.17±0.14 vs 1.00±0.25, p=0.59) and *Ccl3* (1.35±0.21 vs 1.00±0.19, p=0.23) were not altered in TG mice, having as control the levels obtained in WT mice. Instead, expression levels from other proinflammatory cytokines were significantly increased in TG mice, compared with WT mice, namely an increase of 156% in *Tnf-α* (2.56±0.46 vs 1.00±0.18, p=0.004), 229% in *IL-6* (3.29±0.47 vs 1.00±0.22, p=0.0002), 78% in *IL-1β* (1.78±0.23 vs 1.00±0.19, p=0.018) and 110% in *iNos* (2.10±0.38 vs 1.00±0.18, p=0.010).

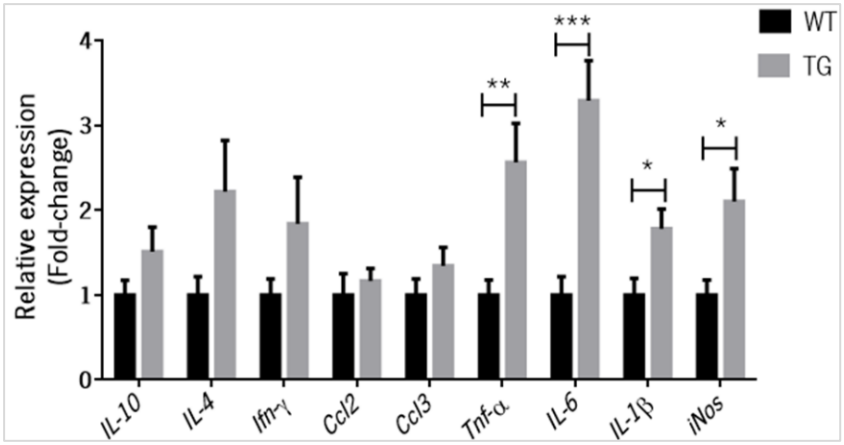


**Figure 20: Transcript' expression analysis of anti- and proinflammatory cytokines at day 7 after mice treatment with BLM.**

Anti-inflammatory (*IL-10*, *IL-4*) and proinflammatory (*Ifn-γ, Ccl2, Ccl3 Tnf-α, IL-6, IL-1β, iNos*) cytokines transcript' were analysed in WT and TG mice lungs by qPCR. Expression levels were normalized to *Gapdh*. Data presented as mean±SEM (*p < 0.05, **p<0.01, ***p<0.001).

As mentioned in the late fibrotic phase of BLM-induced lung fibrosis Tgf-β, Igf-1 and Ctgf are characterized as profibrotic. Although little is known about their function during initial lung injury and repair, there are already some evidences showing a contrary role in relation to their function in the fibrotic phase [122,123,124]. To understand whether the expression of these growth factors is altered in the inflammatory phase, at day 7 post-BLM administration the expression levels from whole lung tissue were determined (Figure 21). We found that expression levels from *Tgf-β1* (0.99±0.02 vs 1.00±0.02, p=0.97) were not altered. However, *Igf-1* (2.60±0.57 vs 1.00±0.22; p=0.013) and *Ctgf* (2.58±0.41 vs 1.00±0.19; p=0.001) were both found to be 160% increase in TG mice, having as control the expression levels obtained in WT mice.

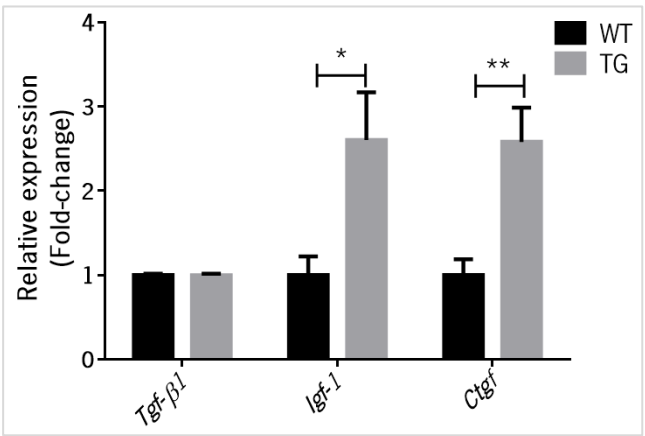


**Figure 21: Transcript' expression analysis of fibrotic-related molecules at day 7 after mice treatment with BLM.**

Fibrotic-related growth factors (*Tgf-β1, Igf-1, Ctgf*) transcript' were analysed in WT and TG mice lungs by qPCR. Expression levels were normalized to *Gapdh*. Data presented as mean±SEM (*p < 0.05, **p<0.01).

These results show that c-Met expression in immune cells impacts on inflammatory influx and infiltration in the tissue with possible involvement of pro-inflammatory cytokines and growth factors.

CHAPTER 5

# DISCUSSION

# 5. Discussion

Idiopathic pulmonary fibrosis is a debilitating lung disorder with a rapid progression and its pathobiology is still not well understood. Currently, it is estimated that these disease affects around 3 million people worldwide and its incidence is rising, as so being vital to find appropriate therapeutic approaches capable of regress or stop the disease progression. Pulmonary fibrosis has specific histological features, being the fibroblastic foci the hallmark that consist in the accumulation of fibroblasts and myofibroblasts. These cells actively participate in tissue remodeling and when this process takes abnormal proportion leads to architectural destruction, loss of function and ultimately death.

Animal models of pulmonary fibrosis have been invaluable for reaching new insights in the disease pathogenesis. The most commonly used in rodents is the BLM-induced model, being clinically relevant, once it mimics human IPF, inducing strong inflammatory reaction, along with release of profibrotic cytokine, collagen production and deposition [125]. The BLM intratracheal administration was chosen once previous studies described a single dose as enough to affect lung architecture in most rodents within short time-frame [93,126]. In case of using a different route of administration relatively higher doses would be needed and the disease progression would be slower [85,86].

BLM-induced lung fibrosis progresses in two phases. The first phase is characterized by pulmonary inflammation consisting in immune cells infiltration, mostly macrophages, neutrophils and lymphocytes, similar to human in which lung damage is followed by the influx of these inflammatory cells [127]. The inflammatory peak in this model is found by day 7, moreover analyses during the first 3 days will reflect the acute injury and inflammatory response to BLM [88].

This phase gradually declines and gives rise to the second phase, closely related with the release of several proinflammatory cytokines and growth factors by lung inflammatory cells infiltrate. These mediators favor activation of key effector cells in tissue remodeling, the fibroblasts and myofibroblasts, culminating in fibrosis as result to extensive collagen deposition [31,93,125]. After a single BLM administration, 14 days is considered the best time point to understand lung fibrotic events since extensive fibrosis is developed, but still with high survival rates compared to 21 days where the ultimate extensive fibrosis occurs [88].

In this thesis the main goal was to understand the influence of c-Met-expressing immune cells in inflammation-associated and fibrogenic process during BLM-induced pulmonary fibrosis. For that, *c-Met*-deletion in immune cells was achieved by using a transgenic mouse approach, where deletion was specifically targeted in the Tie2 lineage, hematopoietic and endothelial cells.

We firstly show that *c-Met* deletion in immune cells plays a protective role against progression of pulmonary fibrosis, since TG mice presented less pronounced weight loss and increased survival compared to WT mice. These findings were clearly associated with the destruction of alveolar parenchyma and increased collagen deposition in the lungs of WT mice compared to TG mice 14 days post-BLM treatment. Moreover, the quantification of hydroxyproline, a key aminoacid in collagen, revealed that the TG group exhibited a decrease trend in collagen content in lung tissue compared to WT mice. The phenomenon of collagen deposition was also observed by analyzing transcript' expression levels of collagen genes (*Col1a1* and *Col1a2*) that were significantly decreased in TG mice. This way, *c-Met* deletion in immune cells significantly ameliorated the long-term effects and the histopathological characteristics BLM-induced lung fibrosis, suggesting that c-Met-expressing immune cells can (dys)regulate pulmonary fibrosis.

As mentioned, the major histological hallmark of this disease is the aberrant fibroblasts' activation and differentiation into myofibroblasts, which exhibit a contractile phenotype because of increased stress fiber formation, α-SMA expression, being the main responsible for abnormal ECM amounts [128]. Thus, our next step was to elucidate possible cellular and molecular effectors behind the lung histological alterations observed in mice with *c-Met*-deleted immune cells. In this way, transcript' expression levels from stromal cell markers and profibrotic mediators were assessed at day 14 after BLM treatment. Notably, TG mice lungs showed a significant reduction in a fibroblast marker expression levels, S100a4, indicating that *c-Met* deletion in immune cells correlate with a decrease of fibroblasts, contributing to an attenuated mesenchymal overgrowth. More analysis should be conducted to confirm the number of these type of cells, namely by flow cytometry or immunofluorescence, using fibroblast (Vimentin, Pdgfr-α, Desmin, Col1a1, S100a4) and myofibroblast markers (α-SMA).

Regarding profibrotic mediators, the mechanisms underlying lung fibroblasts differentiation into myofibroblasts remain poorly understood. Tgf-β1 overexpression is clearly described to increase the accumulation of myofibroblast [129,130]. However, no differences in the transcript' levels of this factor were found, indicating that c-Met regulation does not target Tgf-β. Nevertheless, other

growth factors with profibrotic effects have been reported, namely Ctgf and Igf-1. Ctgf is chemotactic and growth factor for fibroblasts and promotes ECM synthesis [37,36]. Also, Igf-1 has been reported to be involved ECM synthesis and in fibroblasts differentiation into myofibroblast during BLM-induced PF, by stimulation of α-SMA expression in fibroblasts [131]. This study comes in accordance with a previous one, also using BLM-induced lung fibrosis that showed that Igf-1 induced survival and migration of fibroblasts, however blockade with Igf-1R antibody inhibited this effects and promoted fibroblast apoptosis and subsequent resolution of pulmonary fibrosis [132]. Although, no difference in *Ctgf* transcript' levels was found, *Igf-1* transcript' levels were reduced in TG mice, pointing toward a regulatory role of c-Met expression in immune cells leading to induction of Igf-1 production. Possibly increased Igf-1 expression' levels in WT mice detected during later stages of disease progression could be facilitated by the increased inflammatory cells infiltrate in this phase or most importantly in an earlier phase. An interesting future approach to better understand which cellular compartments are contributing for these mediators' production, namely Igf-1, would be to cell sort the main cell populations involved in fibrosis, as epithelial, mesenchymal and immune cells, to evaluate their expression.

Taking in consideration the results obtained in the fibrotic phase, our second aim was to clarify the impact of c-Met expression in immune cells during inflammation-associated fibrosis namely in tissue damage and inflammatory recruitment. Once BLM model is initiated by DNA break [89], cells may undergo necrosis and release intracellular contents into the extracellular space which lead to an exacerbated inflammatory response, leading to increased cell damage and this cycle is associated with reactive oxygen species overproduction causing pulmonary toxicity [90], associated with LDH release into the supernatant. As so, the levels of LDH activity were measured in BALF and tissue homogenate supernatant, showing a reduction in TG mice, indicating less tissue injury and cell damage possibly due to the presence of less inflammatory cells and to their efficient clearance of cellular debris.

Thus, to elucidate the inflammation-associated reaction, the different inflammatory cell populations were analysed at 3 and 7 days after BLM administration, to more closely mimic the inflammatory component of human IPF, which have a role in the initial inflammatory cascade that culminates in lung fibrosis [93]. As previously mentioned, human IPF is associated with chronic inflammation with recruitment of macrophages, neutrophils, and lymphocytes into the airways [127,133], indicating the importance of these populations during disease progression. Neutrophil recruitment

is an important predictor of early mortality in IPF patients [62], their infiltration characterizes the alveolitis inherent to IPF, accompanied with high levels of NE within lung parenchyma [65], which induces both fibroblast proliferation and myofibroblast differentiation *in vitro* [66]. Similarly to human, BLM is described to directly stimulate alveolar macrophages and promote the release of proinflammatory cytokines [134], also representing a prominent cell type in fibrotic process. In fact, inactivation of a specific set of macrophages, consisting mainly in inflammatory activated macrophages, lead to increased survival and diminished collagen deposition in lung injury after BLM administration suggesting an important role for these cells in the disease pathogenesis [135]. Despite representing a relatively small population in a normal lung, T lymphocytes accumulate when pulmonary inflammation and fibrosis occur [136]. Taking these evidences in consideration we characterized the inflammatory influx to the BLM-treated lungs for these target cell populations. We found that *c-Met* deletion in immune cells resulted in reduced number of monocytic-derived resident macrophages and neutrophils in the lungs by day 7 after BLM injection.

Comparing the inflammatory influx at day 3 with the one at day 7, we observed in both animal' groups an increased influx of alveolar macrophages/dendritic cells and monocytic-derived resident macrophages. Interestingly, only the WT group showed an increased number of neutrophils and T cells, confirming that inflammatory influx is attenuated in TG mice, possibly culminates in ameliorated inflammatory and fibrotic responses.

Finisguerra *et al.* previously reported that c-Met is crucial for the neutrophil transmigration across an activated endothelium to the site of inflammation and to reinforce their cytotoxic activity upon HGF stimulation, demonstrating that mice with *c-Met* deletion in Tie2 lineage present lower recruitment of neutrophils to inflamed tumors [97]. Likewise, our results show reduced neutrophils recruitment upon *c-Met* expression deletion as well as reduced tissue cytotoxic levels.

Since there are different lung macrophage resident populations, as alveolar and interstitial, it would be important to better define them. So, in the future it should be interesting to include an alveolar macrophage-specific marker, the Siglec F, which will allow to defined tissue-resident alveolar macrophages by high expression of Siglec F, monocytic-derived alveolar macrophages by low expression and interstitial macrophages by lack of expression [67].

Our studies on inflammatory and fibrotic-related cytokines expression levels during inflammatory phase (7 days after BLM administration), showed an increase of *Tnf-α* levels in TG mice. Taking into account the lower monocytic-derived resident macrophages recruitment on them,

a downregulation of Tnf-α would be expected, as macrophages represent one of the major sources of this cytokine [137]. However, macrophages can be categorized in two main groups: M1-like known to be involved in production of ECM degrading MMPs, proinflammatory cytokines and myofibroblasts apoptosis during disease, identified by its proinflammatory behavior and the synthesis of iNos, IL-1β, and Tnf-α; and M2-like macrophages that are involved in the aberrant wound-healing cascade during fibrosis because their production of TIMPs and profibrotic cytokines, such as IL-4, Tgf-β and IL-10 [55,68]. Moreover, regarding Tnf-α, besides its major proinflammatory, tissue-destructive role several reports suggested Tnf-α as resolution- and repair-enhancer by different mechanisms. Interestingly in an initial phase of disease progression it has been reported to exert antifibrotic effects, to accelerate resolution of established pulmonary fibrosis by decreasing M2 macrophages [138], also stimulating the Igf-1 production with consequent epithelial cell proliferation [122]. Similarly, alveolar macrophage-derived Tnf-α augments alveolar epithelial cell proliferation and re-epithelialization [139]. Redente *et al.* showed that pulmonary delivery of Tnf-α to WT mice with BLM-established pulmonary fibrosis was found to reduce their fibrotic burden, to improve lung function and architecture, to reduce the number and altered the status of profibrotic alternatively activated macrophages towards M1-like phenotype [138]. In the same study they have shown that Tnf-α-deficient mice presented an impaired resolution of fibrosis, associated with the persistence of M2 macrophages and a failure to up-regulate iNos, characteristic of M1-like phenotype.

In accordance with all these evidences, significantly higher expression of M1-associated cytokines, Tnf-α, as already mentioned, but also, IL-6, IL-1β and iNos was observed in BLM-treated *c-Met*-deleted animals. These proinflammatory cytokines suggest an activation towards M1-like phenotype. These results suggest that, although in lower number, M1-like macrophages might be the predominant population during the inflammation-associated fibrosis phase in TG mice, corresponding to the inflammatory and early proliferative phase, possibly leading re-epithelialization of injured lung. In this way, it would be interesting to better characterize these populations in our model, including markers related to each activation phenotype, such as CD80, CD86, iNos for M1 and CD206, Fizz1, Arg1 for M2.

Similarly to our findings some studies associated protection against BLM-induced fibrosis with an increased M1-macrophages phenotype. For example, Ballinger *et al.* used mice deficient in IRAK-M which displayed diminished collagen deposition in association with higher expression of

classically activated macrophage markers. Moreover, Gharib *et al.* using MMP28 knockout mice showed that mice are protected against BLM-induced, presenting less collagen deposition, being this result associated with an increased M1-related cytokines [140,141]. Taking these studies in consideration we can understand that the fact of having increased proinflammatory cytokines expression might be result of M1-like macrophages response.

Kral *et al.* showed that myeloid PTEN-deficient mice present augmented collagen deposition, leading to enhanced morbidity and decreased survival, through reduced numbers of macrophages and T-cells in response to BLM [73], associated with an elevated expression and release of the profibrotic cytokines IL-6 and Tnf-α. Moreover, similar results were obtained by Han *et al.* showing that Psgl-1-deficient mice exhibited enhanced collagen accumulation, resulting in accelerated morbidity and declined survival rate, also showing decreased number of macrophages and T-cells and enhanced cytokines secretion [142]. Contrarily to our results, both studies related more severe pulmonary fibrosis with less macrophages and T-cells recruitment and subsequent increase of cytokines secretion. However, in our results the T-cells recruitment does not seem to be affected, which could be leading to different disease outcomes.

Our data demonstrated that, *Igf-1* and *Ctgf* expression was increased at the inflammatory phase of the disease progression (7 days after BLM administration) in TG mice. These findings come in agreement with some studies demonstrating that these growth factors could have opposite roles depending on the time course of the disease. Indeed, it has been described that in the presence of inflammation or without the premature high levels expression of Tgf-β, Igf-1 production lead to enhanced epithelial cell proliferation and to the absence of chronically denuded alveolar basement membranes, which together result in a constant repair process [122]. Furthermore in skeletal muscle regeneration, Igf-1 produced by monocyte/macrophage has also been described as a potent enhancer of tissue regeneration and suggested to allow for further polarization of macrophages [123]. Regarding Ctgf it is a well-known player downstream Tgf-β, however once Tgf-β is not altered the results suggest that Ctgf is not acting as profibrotic, instead it is described that the early, transient upregulation of Ctgf in the wound repair process promotes normal repair and is necessary to maintain an appropriate angiogenic process within wounds, meaning that when Ctgf expression is confined to early tissue repair, it serves a pro-reparative role [124].

Regarding the transgenic mouse model used, it does not allow a deletion specifically in immune cells, since c-Met expression is also targeted on endothelial cells. However, the vascular

compartment has not been demonstrated as relevant in BLM-induced pulmonary fibrosis progression. Furthermore, c-Met expression in endothelial cells during pulmonary fibrosis has not been reported. In this way, we consider that endothelial cells are not significantly interfering with our results. Having this in mind, to consolidate our results two strategies might be used in the future: chimeric WT mice with transplantation of TG mice bone-marrow or LysM-Cre line that expresses Cre recombinase in the myeloid lineage, along with *c-Met*-floxed line. Moreover, considering that our results suggest a possible regulation of c-Met through expression in neutrophils and/or macrophages, it would be interesting to use specific transgenic for *c-Met*-floxed in both compartments, for example Mrp8-Cre and/or Csf1r-Cre, Cx3CR1-Cre, CD68-Cre transgenic mice, respectively. In addition, as a cue of which cell type c-Met could be inducing the fibrotic phenotype, its expression might be evaluated in the different immune cells and endothelial cells, by flow cytometry or qPCR.

In conclusion, the *c-Met* deletion in immune cells lead to a reduction of neutrophils and monocytic-derived resident macrophages, which hold a M1-like phenotype, and the increase of Ctgf and Igf-1 during inflammatory phase, possibly resulting in improved and more controlled repair process, with consequent fibrogenic processes attenuation, through reduced production of Igf-1, and improved fibrosis disease outcome.

CHAPTER 6

# CONCLUSIONS AND FUTURE PERSPECTIVES

# 6. Conclusions and Future Perspectives

Despite extensive research efforts to unravel the complex and heterogeneous processes underlying IPF pathogenesis, it remains elusive, with no effective treatment available, reflecting a significant health burden.

In this work the main goal was to bring out the influence of c-Met-expressing immune cells in BLM-induced pulmonary fibrosis. Using a transgenic mouse model that allow the *c-Met*-deletion in hematopoietic and endothelial cells, we were capable to observe that the absence of c-Met in these cells highly protected from BLM-induced pulmonary fibrosis. c-Met expression in immune cells leads to lower survival, through (dys)regulation of fibrosis probably through effects on inflammatory processes. These results propose that c-Met inhibition might be beneficial as treatment in maximizing anti-fibrotic outcomes and slowing down disease progression.

In the future, it will be important to clearly distinguish through which immune cells is c-Met conducting the disease progression, with the use of transgenic mouse models for *c-Met* depletion specifically in neutrophils or macrophages. Moreover, characterization with specific markers of activation state of macrophages should be done. Furthermore, it would be interesting to study the cellular accumulation of matrix-producing cells indicative of disease severity, as fibroblasts and myofibroblasts. In addition, it would be important to better understand whether macrophages are the main drivers of c-Met effects in fibrosis, namely through Igf-1 production.

Finally, to understand whether c-Met inhibition would be a valid and effective therapy for IPF patients, it would important to clarify the c-Met expression in neutrophils and/or macrophages present in lung sections from these patients. Afterward, once confirmed, cell-specific delivery of available inhibitors of c-Met used in clinical practice based on the use of nanoparticles approach could be tested in mice with BLM-induced pulmonary fibrosis.

In brief, these thesis findings are opening new avenues for the progress of new therapeutic approaches in IPF.

CHAPTER 7

# REFERENCES

# 7. References


1. Shi, J. *et al.* KLF2 attenuates bleomycin-induced pulmonary fibrosis and inflammation with regulation of AP-1. *Biochem. Biophys. Res. Commun.* **495,** 20–26 (2018).

2. Thannickal, V. J., Toews, G. B., White, E. S., Lynch III, J. P. & Martinez, F. J. Mechanisms of Pulmonary Fibrosis. *Annu. Rev. Med.* **55,** 395–417 (2004).

3. Martinez, F. J. *et al.* Idiopathic pulmonary fibrosis. *Nat. Rev. Dis. Prim.* **3,** 17074 (2017).

4. Raghu, G. *et al.* An Official ATS/ERS/JRS/ALAT Statement: Idiopathic pulmonary fibrosis: Evidence-based guidelines for diagnosis and management. *Am. J. Respir. Crit. Care Med.* **183,** 788–824 (2011).

5. Vancheri, C. & Du Bois, R. M. A progression-free end-point for idiopathic pulmonary fibrosis trials: Lessons from cancer. *Eur. Respir. J.* **41,** 262–269 (2013).

6. Vancheri, C., Failla, M., Crimi, N. & Raghu, G. Idiopathic pulmonary fibrosis: A disease with similarities and links to cancer biology. *Eur. Respir. J.* **35,** 496–504 (2010).

7. Kim, H. J., Perlman, D. & Tomic, R. Natural history of idiopathic pulmonary fibrosis. *Respir. Med.* **109,** 661–670 (2015).

8. Tashiro, J. *et al.* Exploring Animal Models That Resemble Idiopathic Pulmonary Fibrosis. *Front. Med.* **4,** 118 (2017).

9. Tzouvelekis, A., Tzilas, V., Papiris, S., Aidinis, V. & Bouros, D. Diagnostic and prognostic challenges in Idiopathic Pulmonary Fibrosis: A patient's "Q and A" approach. *Pulm. Pharmacol. Ther.* **42,** 21–24 (2017).

10. Aiello, M. *et al.* The earlier, the better: Impact of early diagnosis on clinical outcome in idiopathic pulmonary fibrosis. *Pulm. Pharmacol. Ther.* **44,** 7–15 (2017).

11. International, S. & Consensus, M. American Thoracic Society/European Respiratory Society International Multidisciplinary Consensus Classification of the Idiopathic Interstitial Pneumonias. *Am. J. Respir. Crit. Care Med.* **165,** 277–304 (2002).

12. Raghu, G., Anstrom, K. J., King, T. E., Lasky, J. A. & Martinez, F. J. Prednisone, azathioprine, and N-acetylcysteine for pulmonary fibrosis. *N. Engl. J. Med.* **366,** 1968–1977 (2012).

13. King, T. E. *et al.* A Phase 3 Trial of Pirfenidone in Patients with Idiopathic Pulmonary Fibrosis. *N. Engl. J. Med.* **370,** 2083–2092 (2014).

14. Conte, E. *et al.* Effect of pirfenidone on proliferation, TGF-β-induced myofibroblast differentiation and fibrogenic activity of primary human lung fibroblasts. *Eur. J. Pharm. Sci.* **58,** 13–19 (2014).

15. Richeldi, L. *et al.* Efficacy and Safety of Nintedanib in Idiopathic Pulmonary Fibrosis. *N. Engl. J. Med.* **370,** 2071–2082 (2014).

16. Hartert, M. *et al.* Lung Transplantation. *Dtsch. Arztebl. Int.* **111,** 107–116 (2014).

17. Lederer, D. J. & Martinez, F. J. Idiopathic Pulmonary Fibrosis. *N. Engl. J. Med.* **378,** 1811–1823 (2018).

18. Tzouvelekis, A., Bonella, F. & Spagnolo, P. Update on therapeutic management of idiopathic pulmonary fibrosis. *Ther. Clin. Risk Manag.* **11,** 359–370 (2015).

19. Chapman, H. A. Disorders of lung matrix remodeling. *J. Clin. Invest.* **113,** 148–157 (2004).

20. King, T. E., Pardo, A. & Selman, M. Idiopathic pulmonary fibrosis. *Lancet* **378,** 1949–1961 (2011).

21. Gross, T. J. & Hunninghake, G. W. Idiopathic Pulmonary Fibrosis. *N. Engl. J. Med.* **345,** 517–525 (2001).

22. Kalluri, R. & Neilson, E. G. Epithelial-mesenchymal transition and its implications for fibrosis. *J. Clin. Invest.* **112,** 1776–1784 (2003).

23. Chen, L. J. *et al.* Bleomycin induced epithelial-mesenchymal transition (EMT) in pleural mesothelial cells. *Toxicol. Appl. Pharmacol.* **283,** 75–82 (2015).

24. Wilson, M. S. & Wynn, T. A. Pulmonary fibrosis: pathogenesis, etiology and regulation. *Mucosal Immunol.* **2,** 103–121 (2009).

25. Rockey, D. C., Bell, P. D. & Hill, J. A. Fibrosis — A Common Pathway to Organ Injury and Failure. *N. Engl. J. Med.* **372,** 1138–1149 (2015).

26. Selman, M., Pardo, A. & Kaminski, N. Idiopathic Pulmonary Fibrosis: Aberrant Recapitulation of Developmental Programs? *PLoS Med.* **5,** e62 (2008).

27. Thiery, J. P., Acloque, H., Huang, R. Y. J. & Nieto, M. A. Epithelial-Mesenchymal Transitions in Development and Disease. *Cell* **139,** 871–890 (2009).

28. Todd, N. W. *et al.* Molecular and cellular mechanisms of pulmonary fibrosis. *Fibrogenesis Tissue Repair* **5,** 11 (2012).

29. Wuyts, W. A. *et al.* The pathogenesis of pulmonary fibrosis: A moving target. *Eur. Respir. J.* **41,** 1207–1218 (2013).

30. Agostini, C. Chemokine/Cytokine Cocktail in Idiopathic Pulmonary Fibrosis. *Proc. Am. Thorac. Soc.* **3,** 357–363 (2006).

31. Wynn, T. Cellular and molecular mechanisms of fibrosis. *J. Pathol.* **214,** 199–210 (2008).

32. Yang, I. V. & Schwartz, D. A. Epigenetics of idiopathic pulmonary fibrosis. *Transl. Res.* **165,** 48–60 (2015).

33. Leask, A. & Abraham, D. J. TGF-beta signaling and the fibrotic response. *FASEB J.* **18,** 816–27 (2004).

34. Kisseleva, T. & Brenner, D. A. Mechanisms of Fibrogenesis. *Exp. Biol. Med.* **233,** 109–122 (2008).

35. Leask, A., Denton, C. P. & Abraham, D. J. Insights into the Molecular Mechanism of Chronic Fibrosis: The Role of Connective Tissue Growth Factor in Scleroderma. *J. Invest. Dermatol.* **122,** 1–6 (2004).

36. Grotendorst, G. R. Connective tissue growth factor: A mediator of TGf-β action on fibroblasts. *Cytokine Growth Factor Rev.* **8,** 171–179 (1997).

37. Lin, C. H. *et al.* CXCL12 induces connective tissue growth factor expression in human lung fibroblasts through the Rac1/ERK, JNK, and AP-1 pathways. *PLoS One* **9,** 1–16 (2014).

38. Bonner, J. C. Regulation of PDGF and its receptors in fibrotic diseases. *Cytokine Growth Factor Rev.* **15,** 255–273 (2004).

39. Wynn, T. A. & Ramalingam, T. R. Mechanisms of fibrosis: therapeutic translation for fibrotic disease. *Nat. Med.* **18,** 1028–1040 (2012).

40. Antoniades, H. N. *et al.* Platelet-derived growth factor in idiopathic pulmonary fibrosis. *J. Clin. Invest.* **86,** 1055–1064 (1990).

41. Yoshida, M. *et al.* A histologically distinctive interstitial pneumonia induced by overexpression of the interleukin 6, transforming growth factor beta 1, or platelet-derived growth factor B gene. *Proc. Natl. Acad. Sci. U. S. A.* **92,** 9570–9574 (1995).

42. Aono, Y. *et al.* Imatinib as a novel antifibrotic agent in bleomycin-induced pulmonary fibrosis in mice. *Am. J. Respir. Crit. Care Med.* **171,** 1279–1285 (2005).

43. Daniels, C. E. *et al.* Imatinib treatment for idiopathic pulmonary fibrosis: Randomized placebo-controlled trial results. *Am. J. Respir. Crit. Care Med.* **181,** 604–610 (2010).

44. Kolb, M., Margetts, P. J., Anthony, D. C., Pitossi, F. & Gauldie, J. Transient expression of IL-1beta induces acute lung injury and chronic repair leading to pulmonary fibrosis. *J. Clin. Invest.* **107,** 1529–1536 (2001).

45. Piguet, P. F., Vesin, C., Grau, G. E. & Thompson, R. C. Interleukin 1 receptor antagonist (IL-1ra) prevents or cures pulmonary fibrosis elicited in mice by bleomycin or silica. *Cytokine* **5,** 57–61 (1993).

46. Giri, S. N., Hyde, D. M. & Hollinger, M. A. Effect of antibody to transforming growth factor beta on bleomycin induced accumulation of lung collagen in mice. *Thorax* **48,** 959–966 (1993).

47. Piguet, P. F., Collart, M. A., Grau, G. E., Kapanci, Y. & Vassalli, P. Tumor necrosis factor/cachectin plays a key role in bleomycin-induced pneumopathy and fibrosis. *J. Exp. Med.* **170,** 655–663 (1989).

48. Skibinski, G. The Role of Hepatocyte Growth Factor/c-met Interactions in the Immune System. *Arch. Immunol. Ther. Exp.* **51,** 277–282 (2003).

49. Wynn, T. A. Integrating mechanisms of pulmonary fibrosis. *J. Exp. Med.* **208,** 1339–1350 (2011).

50. Bringardner, B. D., Baran, C. P., Eubank, T. D. & Marsh, C. B. The Role of Inflammation in the Pathogenesis of Idiopathic Pulmonary Fibrosis. *Antioxid. Redox Signal.* **10,** 287–302 (2008).

51. Cui, Y. *et al.* Oxidative stress contributes to the induction and persistence of TGF-β1 induced pulmonary fibrosis. *Int. J. Biochem. Cell Biol.* **43,** 1122–1133 (2011).

52. Xie, H. *et al.* Paraquat-induced pulmonary fibrosis starts at an early stage of inflammation in rats. *Immunotherapy* **4,** 1809–1815 (2012).

53. Chua, F. *et al.* Mice Lacking Neutrophil Elastase Are Resistant to Bleomycin-Induced Pulmonary Fibrosis. *Am. J. Pathol.* **170,** 65–74 (2007).

54. Baran, C. P. *et al.* Important Roles for Macrophage Colony-stimulating Factor, CC Chemokine Ligand 2, and Mononuclear Phagocytes in the Pathogenesis of Pulmonary Fibrosis. *Am. J. Respir. Crit. Care Med.* **176,** 78–89 (2007).

55. Kolahian, S., Fernandez, I. E., Eickelberg, O. & Hartl, D. Immune mechanisms in pulmonary fibrosis. *Am. J. Respir. Cell Mol. Biol.* **55,** 309–322 (2016).

56. Parambil, J. G., Myers, J. L. & Ryu, J. H. Histopathologic Features and Outcome of Patients With Acute Exacerbation of Idiopathic Pulmonary Fibrosis Undergoing Surgical Lung Biopsy. *Chest* **128,** 3310–3315 (2005).

57. Kruger, P. *et al.* Neutrophils: Between Host Defence, Immune Modulation, and Tissue Injury. *PLoS Pathog.* **11,** 1–22 (2015).

58. Takemasa, A., Ishii, Y. & Fukuda, T. A neutrophil elastase inhibitor prevents bleomycin-induced pulmonary fibrosis in mice. *Eur. Respir. J.* **40,** 1475–1482 (2012).

59. Taooka, Y., Maeda, A., Hiyama, K., Ishioka, S. & Yamakido, M. Effects of neutrophil elastase inhibitor

on bleomycin-induced pulmonary fibrosis in mice. *Am. J. Respir. Crit. Care Med.* **156,** 260–265 (1997).

60. Pardo, A. *et al.* Increase of Lung Neutrophils in Hypersensitivity Pneumonitis Is Associated with Lung Fibrosis. *Am. J. Respir. Crit. Care Med.* **161,** 1698–1704 (2000).

61. Yasuoka, S. *et al.* Comparison of cell profiles of bronchial and bronchoalveolar lavage fluids between normal subjects and patients with idiopathic pulmonary fibrosis. *Tohoku J. Exp. Med.* **146,** 33–45 (1985).

62. Kinder, B. W. *et al.* Baseline BAL neutrophilia predicts early mortality in idiopathic pulmonary fibrosis. *Chest* **133,** 226–232 (2008).

63. Tabuena, R. P. *et al.* Cell Profiles of Bronchoalveolar Lavage Fluid as Prognosticators of Idiopathic Pulmonary Fibrosis/Usual Interstitial Pneumonia among Japanese Patients. *Respiration* **72,** 490–498 (2005).

64. Hunninghake, G. W., Gadek, J. E., Lawley, T. J. & Crystal, R. G. Mechanisms of neutrophil accumulation in the lungs of patients with idiopathic pulmonary fibrosis. *J. Clin. Invest.* **68,** 259–269 (1981).

65. Obayashi, Y. *et al.* The role of neutrophils in the pathogenesis of idiopathic pulmonary fibrosis. *Chest* **112,** 1338–1343 (1997).

66. Gregory, A. D. *et al.* Neutrophil elastase promotes myofibroblast differentiation in lung fibrosis. *J. Leukoc. Biol.* **98,** 143–152 (2015).

67. Misharin, A. V. *et al.* Monocyte-derived alveolar macrophages drive lung fibrosis and persist in the lung over the life span. *J. Exp. Med.* **214,** 2387–2404 (2017).

68. Byrne, A. J., Mathie, S. A., Gregory, L. G. & Lloyd, C. M. Pulmonary macrophages: key players in the innate defence of the airways. *Thorax* **70,** 1189–1196 (2015).

69. Duffield, J. S. *et al.* Selective depletion of macrophages reveals distinct, opposing roles during liver injury and repair. *J. Clin. Invest.* **115,** 56–65 (2005).

70. Piguet, P. F., Rosen, H., Vesin, C. & Grau, G. E. Effective Treatment of the Pulmonary Fibrosis Elicited in Mice by Bleomycin or Silica with Anti-CD-11 Antibodies. *Am. Rev. Respir. Dis.* **147,** 435–441 (1993).

71. Barron, L. & Wynn, T. A. Fibrosis is regulated by Th2 and Th17 responses and by dynamic interactions between fibroblasts and macrophages. *Am. J. Physiol. Liver Physiol.* **300,** G723–G728 (2011).

72. Wynn, T. A. & Vannella, K. M. Macrophages in Tissue Repair, Regeneration, and Fibrosis. *Immunity* **44,** 450–462 (2016).

73. Kral, J. B. *et al.* Sustained PI3K Activation exacerbates BLM-induced Lung Fibrosis via activation of pro-inflammatory and pro-fibrotic pathways. *Sci. Rep.* **6,** 23034 (2016).

74. Sharma, S. K., MacLean, J. A., Pinto, C. & Kradin, R. L. The effect of an anti-CD3 monoclonal antibody on bleomycin-induced lymphokine production and lung injury. *Am. J. Respir. Crit. Care Med.* **154,** 193–200 (1996).

75. Keane, M. P., Belperio, J. A., Burdick, M. D. & Strieter, R. M. IL-12 attenuates bleomycin-induced pulmonary fibrosis. *Am. J. Physiol. Cell. Mol. Physiol.* **281,** L92–L97 (2001).

76. Saito, A., Okazaki, H., Sugawara, I., Yamamoto, K. & Takizawa, H. Potential action of IL-4 and IL-13 as fibrogenic factors on lung fibroblasts in vitro. *Int. Arch. Allergy Immunol.* **132,** 168–176

(2003).

77. Wynn, T. A. Fibrotic disease and the TH1/TH2 paradigm. *Nat. Rev. Immunol.* **4,** 583–594 (2004).

78. Luzina, I. G., Todd, N. W., Iacono, A. T. & Atamas, S. P. Roles of T lymphocytes in pulmonary fibrosis. *J. Leukoc. Biol.* **83,** 237–244 (2007).

79. Bucala, R., Spiegel, L. A., Chesney, J., Hogan, M. & Cerami, A. Circulating fibrocytes define a new leukocyte subpopulation that mediates tissue repair. *Mol. Med.* **1,** 71–81 (1994).

80. Strieter, R. M., Keeley, E. C., Hughes, M. A., Burdick, M. D. & Mehrad, B. The role of circulating mesenchymal progenitor cells (fibrocytes) in the pathogenesis of pulmonary fibrosis. *J. Leukoc. Biol.* **86,** 1111–1118 (2009).

81. Ebihara, Y. *et al.* Hematopoietic origins of fibroblasts: II. In vitro studies of fibroblasts, CFU-F, and fibrocytes. *Exp. Hematol.* **34,** 219–229 (2006).

82. Madala, S. K. *et al.* Bone Marrow–Derived Stromal Cells Are Invasive and Hyperproliferative and Alter Transforming Growth Factor-α–Induced Pulmonary Fibrosis. *Am. J. Respir. Cell Mol. Biol.* **50,** 777–786 (2014).

83. Moeller, A. *et al.* Circulating fibrocytes are an indicator of poor prognosis in idiopathic pulmonary fibrosis. *Am. J. Respir. Crit. Care Med.* **179,** 588–594 (2009).

84. Hashimoto, N., Jin, H., Liu, T., Chensue, S. W. & Phan, S. H. Bone marrow–derived progenitor cells in pulmonary fibrosis. *J. Clin. Invest.* **113,** 243–252 (2004).

85. Moore, B. B. & Hogaboam, C. M. Murine models of pulmonary fibrosis. *Am. J. Physiol. Lung Cell. Mol. Physiol.* **294,** L152–L160 (2008).

86. Moore, B. B. *et al.* Animal models of fibrotic lung disease. *Am. J. Respir. Cell Mol. Biol.* **49,** 167–179 (2013).

87. Reinert, T., Baldotto, C. S. R., Nunes, F. A. P. & Scheliga, A. A. S. Bleomycin-Induced Lung Injury. *J. Cancer Res.* **2013,** 1–9 (2013).

88. Moeller, A., Ask, K., Warburton, D., Gauldie, J. & Kolb, M. The bleomycin animal model: A useful tool to investigate treatment options for idiopathic pulmonary fibrosis? *Int. J. Biochem. Cell Biol.* **40,** 362–382 (2008).

89. Claussen, C. A. & Long, E. C. Nucleic Acid Recognition by Metal Complexes of Bleomycin. *Chem. Rev.* **99,** 2797–2816 (1999).

90. Chaudhary, N. I., Schnapp, A. & Park, J. E. Pharmacologic differentiation of inflammation and fibrosis in the rat bleomycin model. *Am. J. Respir. Crit. Care Med.* **173,** 769–776 (2006).

91. Walters, D. M. & Kleeberger, S. R. Mouse Models of Bleomycin-Induced Pulmonary Fibrosis. in *Current Protocols in Pharmacology* **Chapter 5,** Unit 5.46 (John Wiley & Sons, Inc., 2008).

92. Wei, Y.-R. *et al.* Establishment of the mouse model of acute exacerbation of idiopathic pulmonary fibrosis. *Exp. Lung Res.* **42,** 75–86 (2016).

93. Izbicki, G., Segel, M. J., Christensen, T. G., Conner, M. W. & Breuer, R. Time course of bleomycin-induced lung fibrosis. *Int. J. Exp. Pathol.* **83,** 111–119 (2002).

94. Chua, F., Gauldie, J. & Laurent, G. J. Pulmonary fibrosis: Searching for model answers. *Am. J. Respir. Cell Mol. Biol.* **33,** 9–13 (2005).

95. Tsou, H. K. *et al.* HGF and c-Met Interaction Promotes Migration in Human Chondrosarcoma Cells. *PLoS One* **8,** e53974 (2013).

96. Rubin, J. Hepatocyte growth factor/scatter factor and its receptor, the c-met proto-oncogene product. *Biochim. Biophys. Acta - Rev. Cancer* **1155,** 357–371 (1993).

97. Finisguerra, V. *et al.* MET is required for the recruitment of anti-tumoural neutrophils. *Nature* **522,** 349–353 (2015).

98. Nakamura, T., Sakai, K., Nakamura, T. & Matsumoto, K. Hepatocyte growth factor twenty years on: Much more than a growth factor. *J. Gastroenterol. Hepatol.* **26,** 188–202 (2011).

99. Ponzetto, C. *et al.* A novel recognition motif for phosphatidylinositol 3-kinase binding mediates its association with the hepatocyte growth factor/scatter factor receptor. *Mol. Cell. Biol.* **13,** 4600–4608 (1993).

100. Ponzetto, C. *et al.* A multifunctional docking site mediates signaling and transformation by the hepatocyte growth factor/scatter factor receptor family. *Cell* **77,** 261–271 (1994).

101. You, W. K. & McDonald, D. M. The hepatocyte growth factor/c-Met signaling pathway as a therapeutic target to inhibit angiogenesis. *BMB Rep.* **41,** 833–839 (2008).

102. Yamamoto, H. *et al.* Epithelial-vascular cross talk mediated by VEGF-A and HGF signaling directs primary septae formation during distal lung morphogenesis. *Dev. Biol.* **308,** 44–53 (2007).

103. Crestani, B. *et al.* Differential role of neutrophils and alveolar macrophages in hepatocyte growth factor production in pulmonary fibrosis. *Lab. Invest.* **82,** 1015–1022 (2002).

104. Stern, J. B. *et al.* Keratinocyte growth factor and hepatocyte growth factor in bronchoalveolar lavage fluid in acute respiratory distress syndrome patients. *Crit. Care Med.* **28,** 2326–2333 (2000).

105. Sakamaki, Y. *et al.* Hepatocyte Growth Factor Stimulates Proliferation of Respiratory Epithelial Cells during Postpneumonectomy Compensatory Lung Growth in Mice. *Am. J. Respir. Cell Mol. Biol.* **26,** 525–533 (2002).

106. Dohi, M., Hasegawa, T., Yamamoto, K. & Marshall, B. Hepatocyte growth factor attenuates collagen accumulation in a murine model of pulmonary fibrosis. *Am. J. Respir. Crit. Care Med.* **162,** 2302–2307 (2000).

107. Mizuno, S., Matsumoto, K., Li, M.-Y. & Nakamura, T. HGF reduces advancing lung fibrosis in mice: a potential role for MMP-dependent myofibroblast apoptosis. *FASEB J.* **19,** 580–582 (2005).

108. Ishizawa, K. *et al.* Hepatocyte growth factor induces angiogenesis in injured lungs through mobilizing endothelial progenitor cells. *Biochem. Biophys. Res. Commun.* **324,** 276–280 (2004).

109. Crestani, B. *et al.* Hepatocyte growth factor and lung fibrosis. *Proc. Am. Thorac. Soc.* **9,** 158–163 (2012).

110. Ware, L. B. & Matthay, M. A. Keratinocyte and hepatocyte growth factors in the lung: roles in lung development, inflammation, and repair. *Am. J. Physiol. Cell. Mol. Physiol.* **282,** L924–L940 (2002).

111. Yaekashiwa, M. *et al.* Simultaneous or delayed administration of hepatocyte growth factor equally represses the fibrotic changes in murine lung injury induced by bleomycin. A morphologic study. *Am. J. Respir. Crit. Care Med.* **156,** 1937–1944 (1997).

112. Yanagita, K. *et al.* Hepatocyte growth factor may act as a pulmotrophic factor on lung regeneration after acute lung injury. *J. Biol. Chem.* **268,** 21212–21217 (1993).

113. Parra, E. R., Kairalla, R. A., Ribeiro de Carvalho, C. R., Eher, E. & Capelozzi, V. L. Inflammatory Cell Phenotyping of the Pulmonary Interstitium in Idiopathic Interstitial Pneumonia. *Respiration* **74,** 159–169 (2007).

114. Glodde, N. *et al.* Reactive Neutrophil Responses Dependent on the Receptor Tyrosine Kinase c-MET

Limit Cancer Immunotherapy. *Immunity* **47,** 789–802.e9 (2017).

115. Galimi, F. *et al.* Hepatocyte Growth Factor Is a Regulator of Monocyte-Macrophage Function. *J. Immunol.* **166,** 1241–1247 (2001).

116. Kurz, S. M. *et al.* The impact of c-met/scatter factor receptor on dendritic cell migration. *Eur. J. Immunol.* **32,** 1832–1838 (2002).

117. Adams, D. H. *et al.* Hepatocyte growth factor and macrophage inflammatory protein 1 beta: structurally distinct cytokines that induce rapid cytoskeletal changes and subset-preferential migration in T cells. *Proc. Natl. Acad. Sci. USA.* **91,** 7144–7148 (1994).

118. Benkhoucha, M. *et al.* Identification of a novel population of highly cytotoxic c-Met-expressing CD8 + T lymphocytes. *EMBO Rep.* **18,** 1545–1558 (2017).

119. Ashcroft, T., Simpson, J. M. & Timbrell, V. Simple method of estimating severity of pulmonary fibrosis on a numerical scale. *J. Clin. Pathol.* **41,** 467–470 (1988).

120. Livak, K. J. & Schmittgen, T. D. Analysis of Relative Gene Expression Data Using Real-Time Quantitative PCR and the 2−ΔΔCT Method. *Methods* **25,** 402–408 (2001).

121. Murray, P. J. & Wynn, T. A. Protective and pathogenic functions of macrophage subsets. *Nat. Rev. Immunol.* **11,** 723–737 (2011).

122. Krein, P. M. & Winston, B. W. Roles for insulin-like growth factor I and transforming growth factor-beta in fibrotic lung disease. *Chest* **122,** 289S–293S (2002).

123. Tonkin, J. *et al.* Monocyte/macrophage-derived IGF-1 orchestrates murine skeletal muscle regeneration and modulates autocrine polarization. *Mol. Ther.* **23,** 1189–1200 (2015).

124. Alfaro, M. P. *et al.* A physiological role for connective tissue growth factor in early wound healing. *Lab. Invest.* **93,** 81–95 (2013).

125. Gasse, P. *et al.* IL-1R1/MyD88 signaling and the inflammasome are essential in pulmonary inflammation and fibrosis in mice. *J. Clin. Invest.* **117,** 3786–3799 (2007).

126. Kim, S. N. *et al.* Dose-response Effects of Bleomycin on Inflammation and Pulmonary Fibrosis in Mice. *Toxicol. Res.* **26,** 217–222 (2010).

127. Janick-Buckner, D., Ranges, G. E. & Hacker, M. P. Alteration of bronchoalveolar lavage cell populations following bleomycin treatment in mice. *Toxicol. Appl. Pharmacol.* **100,** 465–473 (1989).

128. Hinz, B. Formation and Function of the Myofibroblast during Tissue Repair. *J. Invest. Dermatol.* **127,** 526–537 (2007).

129. Ji, H. *et al.* Rho/Rock cross-talks with transforming growth factor-β/Smad pathway participates in lung fibroblast-myofibroblast differentiation. *Biomed. reports* **2,** 787–792 (2014).

130. Lee, C. G. Transgenic Modeling of Transforming Growth Factor- 1: Role of Apoptosis in Fibrosis and Alveolar Remodeling. *Proc. Am. Thorac. Soc.* **3,** 418–423 (2006).

131. Hung, C. F., Rohani, M. G., Lee, S.-S., Chen, P. & Schnapp, L. M. Role of IGF-1 pathway in lung fibroblast activation. *Respir. Res.* **14,** 102 (2013).

132. Choi, J.-E. *et al.* Insulin-like Growth Factor-I Receptor Blockade Improves Outcome in Mouse Model of Lung Injury. *Am. J. Respir. Crit. Care Med.* **179,** 212–219 (2009).

133. Ward, P. A. & Hunninghake, G. W. Lung Inflammation and Fibrosis. *Crit. Care Med.* **157,** 123–129 (1998).

134. Jordana, M., Richards, C., Irving, L. B. & Gauldie, J. Spontaneous in vitro release of alveolar-macrophage cytokines after the intratracheal instillation of bleomycin in rats. Characterization and kinetic studies. *Am Rev Respir Dis* **137,** 1135–1140 (1988).

135. Nagai, T. *et al.* Effect of an immunotoxin to folate receptor on bleomycin-induced experimental pulmonary fibrosis. *Clin. Exp. Immunol.* **161,** 348–356 (2010).

136. Lo Re, S., Lison, D. & Huaux, F. CD4 + T lymphocytes in lung fibrosis: diverse subsets, diverse functions. *J. Leukoc. Biol.* **93,** 499–510 (2013).

137. Piguet, P. F., Ribaux, C., Karpuz, V., Grau, G. E. & Kapanci, Y. Expression and localization of tumor necrosis factor-alpha and its mRNA in idiopathic pulmonary fibrosis. *Am. J. Pathol.* **143,** 651–655 (1993).

138. Redente, E. F. *et al.* Tumor necrosis factor-α accelerates the resolution of established pulmonary fibrosis in mice by targeting profibrotic lung macrophages. *Am. J. Respir. Cell Mol. Biol.* **50,** 825–837 (2014).

139. Cakarova, L. *et al.* Macrophage tumor necrosis factor-α induces epithelial expression of granulocyte-macrophage colony-stimulating factor: Impact on alveolar epithelial repair. *Am. J. Respir. Crit. Care Med.* **180,** 521–532 (2009).

140. Ballinger, M. N. *et al.* IRAK-M promotes alternative macrophage activation and fibroproliferation in bleomycin-induced lung injury. *J. Immunol.* **194,** 1894–1904 (2015).

141. Gharib, S. A. *et al.* MMP28 promotes macrophage polarization toward M2 cells and augments pulmonary fibrosis. *J. Leukoc. Biol.* **95,** 9–18 (2014).

142. Han, X. & Wang, S. Deficiency of Psgl-1 accelerates bleomycin (BLM)-induced lung fibrosis and inflammation in mice through activating PI3K/AKT. *Biochem. Biophys. Res. Commun.* **491,** 558–565 (2017).